Session 5

CONTAINMENT VENTING

MONDAY: October 20, 1980
CHAIRMAN: Robert Hilliard
Hanford Engineering Lab

DEVELOPMENT OF A PASSIVE, SELF-CLEANING SCRUBBER FOR CONTAINMENT VENTING APPLICATIONS

R. K. Owen and A. K. Postma
Hanford Engineering Development Laboratory
Operated by Westinghouse Hanford Company
Richland, Washington 99352

Abstract

A novel air cleaning concept is being developed at the Hanford Engineering Development Laboratory for potential use in venting reactor containment buildings. The two-stage system employs a pre-scrubber (a submerged gravel scrubber) and a fibrous scrubber to obtain high removal efficiencies for particulate contaminants. The submerged gravel scrubber is unique in that water flow is induced by the gas flow, eliminating the need for an active liquid pump. In addition, design gas velocities through the gravel bed are 10 to 20 times higher than for a conventional sand bed filter.

A series of development tests have been performed on an engineering scale model with a gravel bed area of 0.07 m^2. Hydraulic tests indicate that the scrubber can be designed to operate at a superficial gas velocity of 0.50 m/s. Aerosol tests were performed with a variety of sodium fire aerosols. The aerosol mass removal efficiency for the pre-scrubber was 99.8% and the efficiency for the system exceeded 99.99%. The test results show that the aerosol removal efficiency is not a strong function of the gas velocity. Scale-up tests were made to evaluate gas distribution on a larger bed. The results demonstrated that the self-cleaning gravel bed can be scaled-up to the sizes required for full-scale containment applications.

I. Background

A DOE-funded program is underway at Hanford Engineering Development Laboratory (HEDL) to develop air cleaning systems which could be employed in containment venting applications in LMFBR plants. An evaluation of alternative air cleaning concepts showed that aqueous scrubbers rated high because of their high aerosol loading capacity, their ability to handle a wide range of thermal conditions, their small size, and their relatively low cost.[1] Subsequently, two and three component systems have been tested at large scale.[2,3]

While the scrubber systems based on commercially available components appear to meet all required design criteria, evaluations of containment venting applications show that an ideal scrubber would be characterized by:

- Passive operation
- High reliability after long standby periods
- Minimal electric power requirements

A passive, high-loading capacity scrubber which needs no external power for venting applications was conceived at HEDL. The scrubber combines the passive features of a sand bed with the low cost and size features of a scrubber which employs active components. This device has been termed a Submerged Gravel Scrubber (SGS).

This scrubbing concept was conceived in 1978 and has been under development since then. A patent application for this device has been filed by the U. S. Department of Energy.

II. Experimental Arrangement

Equipment Description

The SGS consists of a bed of gravel submerged in a pool of water as shown in Figure 1. Gas laden with aerosol is drawn down a central inlet duct to the bottom of the bed where the gas distributes itself across the bed. The gas subsequently flows upward through small irregular channels formed in the packing interstices. Aerosol is removed from the gas primarily by interception, diffusional, and inertial forces.

The gas in the interstices reduces the apparent density of the liquid inside the bed. Consequently, water outside the bed flows into the packing, upward, and spills over the top. The collected aerosol is continuously washed from the gravel. The novel feature of this device is the passive, self-cleaning bed.

Gas leaving the submerged bed may be further cleaned of aerosols by placing a High Efficiency Fiber Demister (HEFD) over the SGS. Gas laden with aerosol that has penetrated the SGS and entrained liquid pass upward through the center of the fiber element and radially outward through the fibers. Aerosol is removed primarily by interception and Brownian diffusion. Liquid mist carried by the gas collects on the fibers and washes the element clean of soluble and insoluble material. The primary function of the HEFD is to remove the smaller sized aerosols.

The SGS concept was tested using a 0.305-m diameter bed (shown in Figure 2). The bed lengths tested were between 0.305-m and 0.610-m. The packed bed was contained in an 0.314-m OD acrylic tube 0.762-m long, supported 15-cm above the bottom of an acrylic tank. The packing was placed inside the tube between an upper and lower support screen. The screen openings were 4.75 mm square.

The packing was crushed basalt rock, hand seived into three fractions: (+) 0.64 cm to (-) 0.95 cm, (+) 0.95 cm to (-) 1.27 cm, and (+) 1.27 cm to (-) 1.59 cm. The material density of the rock was 2.84 g/cm^3. The typical void fraction of a packed bed using the middle fraction was 0.45 ± 0.05. The rock was characterized as having no smooth sides.

A 6.4-cm OD pipe inserted through the center of the bed served as a gas inlet duct. The remaining bed surface area was 0.070-m^2. The bed was placed inside a 0.78-m square tank 0.93-m deep. The tank was fitted with a 0.76-m high lid. The nominal liquid operating level was even with the top support screen and the liquid volume was 445

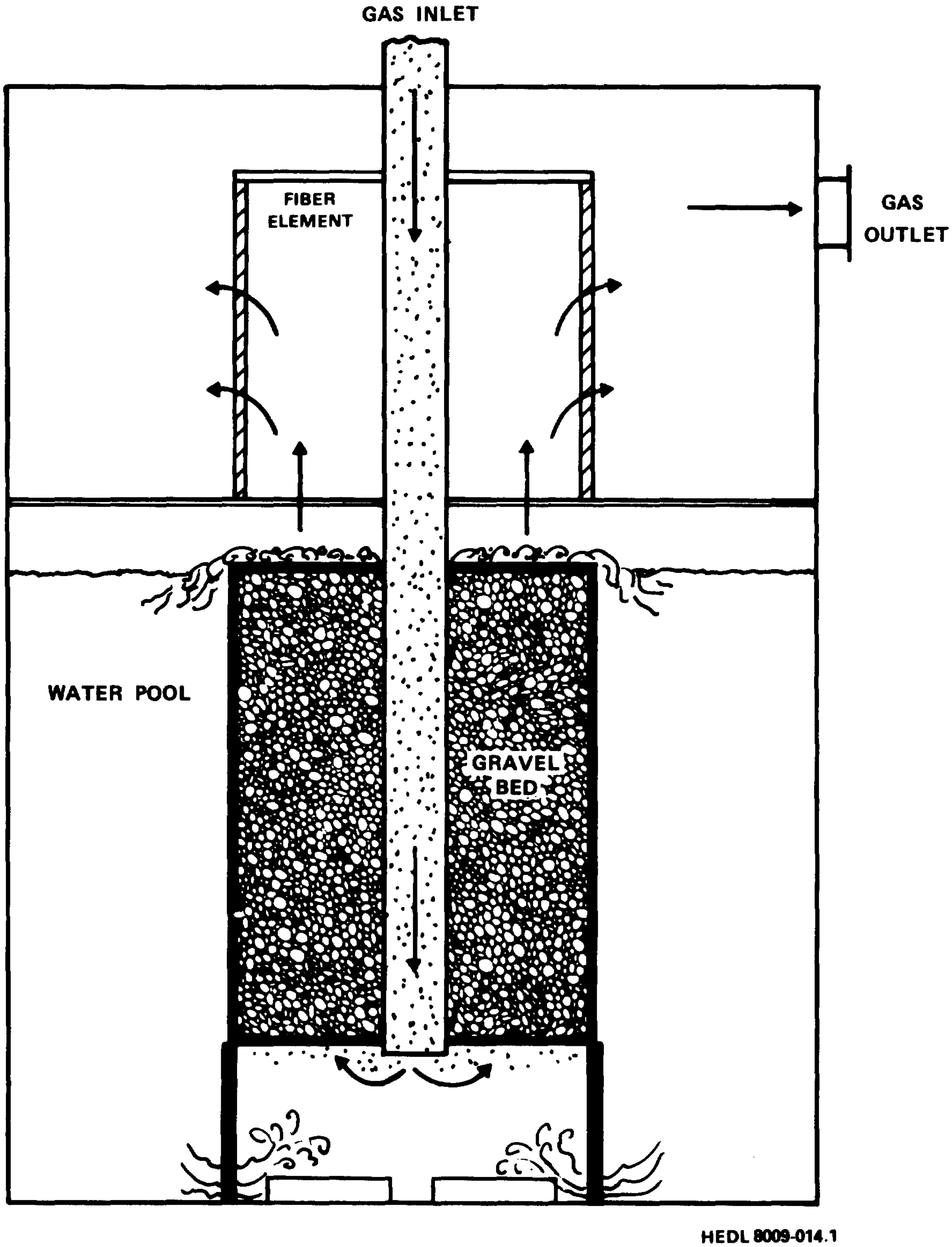

Figure 1. Schematic of Submerged Gravel Scrubber.

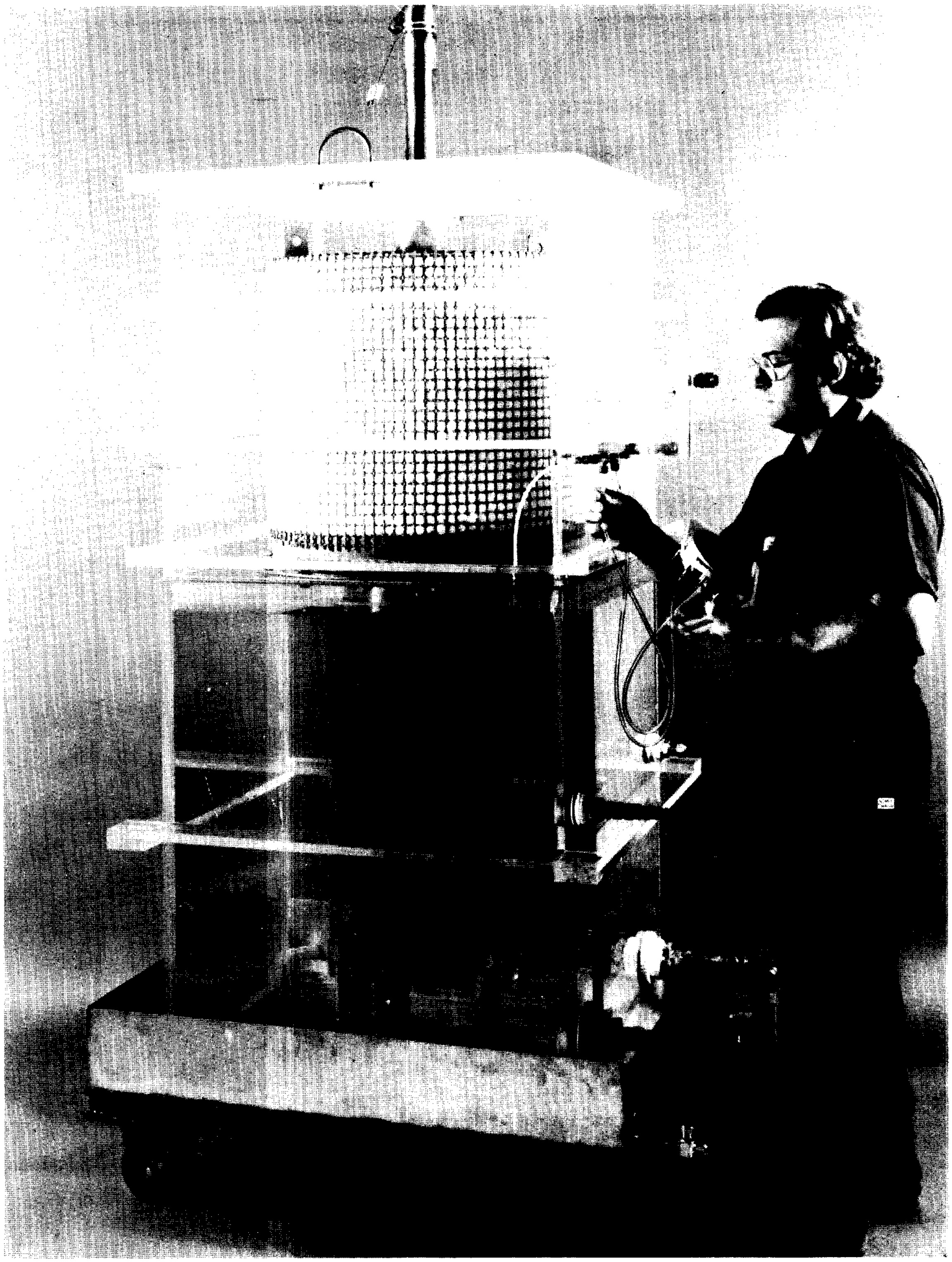

Figure 2. Experimental Scrubber.

liters.

The HEFD was a polypropylene H-E series Brink Mist Eliminator*, Type 2424 RFUSD Flow. This was bolted to a tube sheet placed between the tank and tank lid. The element was a hollow cylinder 0.6-m long by 0.61-m OD. The element consists of 20 μm diameter fibers packed between two galvanized screens to form the 7.6 cm thick wall of the cylinder. The void fraction of the fiber was calculated to be 85%. The unit is sized for maximum flow of 0.09 m^3/s.

A blower was used to induce gas flow at rates between 0.002 and 0.035 m^3/s. Gas flowed from the aerosol source, through the SGS and HEFD, through a back-up HEPA filter, through an orifice, and then through the blower.

The base case bed configuration was a 0.61-m deep bed of (+) 0.95-cm to (-) 1.27 cm rock, constrained between two screen supports. The inlet duct was installed with the duct end 1.3-cm below the bottom support screen. The packing tube projected below the bottom support screen to form a 13-cm skirt. The operating liquid level was even with the top screen support.

Test Aerosol Generation and Sampling

Test aerosol was generated in two separate test facilities. Three tests were performed using aerosol generated by a sodium pool fire in a 1 m^2 heated pan located in a 330 m^3 volume closed concrete room. The generated aerosol was drawn through 7 meters of 10-cm diameter duct to the scrubber. A fourth test was performed in this facility using aerosols generated by a lithium pool fire.

The remaining tests were made using sodium aerosols generated by spray fires in a 7.6-m diameter, 850-m^3 vessel. The test aerosol was generated as part of an air cleaning development program.[2,3] Liquid sodium was continuously sprayed through nozzles located at the vessel bottom. Steam and CO_2 gas were fed to the vessel at controlled rates. Aerosol laden gas was pulled from the vessel through lines varying between 3-m to 7-m long of 10-cm diameter duct to the scrubber.

Aerosol samples (filters and cascade impactors) were taken from the inlet duct immediately preceding the scrubber, the gas space between the SGS and the HEFD, and the entrance to the outlet duct. Liquid samples were periodically withdrawn from the tank. The aerosol mass concentration was determined gravimetrically and the sodium concentration was determined by acid titrimetry. Lower levels of sodium on the cascade impactor stages and downstream filters were determined by emission spectroscopy. Blank corrections were made to account for background sodium in the filter media and demineralized water. The backup HEPA filter was destructively leached after each test and the solution analyzed for sodium. Cascade impactors were used for particle size measurement and electron microscope grids were exposed for particle shape information.

* Monsanto Enviro-Chem Systems, Inc., St. Louis, Missouri 63141

Experimental Procedure

Two sets of tests were made on the SGS; hydraulic tests and efficieny tests. Hydraulic tests were made to investigate the effect of various design and operating parameters on the scrubber pressure drop and liquid pumping rate. Efficiency tests were made using aerosols to determine the aerosol penetrations for different bed configurations and operating conditions.

Hydraulic tests were made using room air. A drain ring was fitted to the top of the packing tube to catch the water that was pumped through the rocks. The liquid pumping rate, scrubber pressure drop, and minimum liquid level at which liquid was pumped through the bed was determined at four gas flowrates for eight bed configurations.

Efficiency tests were made using aerosols generated by liquid metal fires. The sodium and lithium pool fires were created by delivering approximately 30 kg of liquid metal at about 200°C to a preheated burn pan. Approximately 30 minutes after the start of the pool fires, gas flow was initiated through the scrubber. Scrubber operation was started about four hours after the start of spray fires, allowing time for aerosol concentration build-up and particle growth.

The test conditions and primary test variables are given in Table I for the hydraulic tests and in Table II for the efficiency tests.

III. Experimental Results

Pressure Drop

The pressure drop across the SGS is approximately equal to the hydraulic head of water. Figure 3 shows the pressure drop as a function of the gas superficial velocity, V_{SG}. At the lowest gas velocities, the SGS pressure drop is equal to the submergence of the inlet duct below the liquid surface. As the gas flowrate increases, a gas layer builds up across the bed bottom. The gas layer thickness oscillates between a maximum thickness, dependent on the gas velocity and zero depth. During the latter, liquid enters the bed and begins to fill the packing interstices. When the gas layer again forms across the bed bottom, the liquid is driven upward through the packing. Thus, the pressure drop and liquid superficial velocity oscillate at a frequency of about 27 cycles per minute for superficial gas velocities between 0.13 and 0.51 m/s. This phenomenon occurs for a variety of blower and duct arrangements, and for both pressure driven gas flow and exhausted gas flow; hence, the oscillatory operation is attributed to the hydraulics of two phase flow through the packed bed.

Figure 3 shows that the pressure drop reaches a maximum and then decreases. At gas velocities greater than 0.5-m/s the gas layer begins to stablize. At velocities beyond about 1.0-m/s the packing will be blown free of liquid and the pressure drop across the packing will increase similarly to a dry packed bed.

The pressure drop across the HEFD is essentially linear with gas flowrate and is 1.1 KPa at 0.03 std m^3/s.

TABLE I. Hydraulic Tests Bed Configurations

Bed Length (cm)	Type of Support	Packing Size (cm)	Inlet Duct Submergence (cm)	Bed Submergence (cm)	Parameter Studied
61.	Screen	(+) 0.95/(-) 1.27	66.	0.	Base Case
61.	Plate	(+) 0.95/(-) 1.27	66.	0.	Type of Support
61.	Plate	(+) 0.95/(-) 1.27	76.	0.	Inlet Duct Submergence
61.	Plate	(+) 0.64/(-) 0.95	66.	0.	Packing Size
46.	Plate	(+) 0.95/(-) 1.27	51.	0.	Bed Height/Inlet Duct Submergence
46.	Plate	(+) 0.95/(-) 1.27	66.	18.	Bed Submergence
61.	Plate (lower only)	(+) 0.95/(-) 1.27	66.	0.	Bed Compression (No top bed support)
46.	Plate	(+) 0.95/(-) 1.27	66.	0.	Bed height
---	-----	----------------	66.	---	No packing

TABLE II. Conditions for Efficiency Tests

Test	Aerosol Source (a)	Dominant Aerosol Form	Test Duration (Hr)	Average Aerosol Concentration (g/m^3, STP)	Superficial Gas Velocity (m/s)
1	Spray Fire, CSTF	Na_2CO_3	9.7	5.5	0.03 - 0.50
2	Pool Fire, LSFF	$Na_2O_2/NaOH$	4.3	9.0	0.02 - 0.37
3	Pool Fire, LSFF	$Na_2O_2/NaOH$	2.7	8.2	0.03 - 0.45
4	Pool Fire, LSFF	$Na_2O_2/NaOH$	4.0	7.5	0.01 - 0.33
5	Spray Fire, CSTF	LiO	2.9	1.0	0.01 - 0.33
6	Spray Fire, LSFF	$NaOH \cdot 2.0H_2O$	24.	9.8	0.28 - 0.45
7	Spray Fire, CSTF	$NaOH \cdot 0.2H_2O$	20.	19.4	0.17 - 0.50
8	Spray Fire, CSTF	$NaOH \cdot 1.0H_2O$	7.4	49.1	0.17 - 0.33

(a) CSTF - Containment System Test Facility; 850 m^3 vessel
LSFF - Large Scale Fire Facility; 330 m^3 room

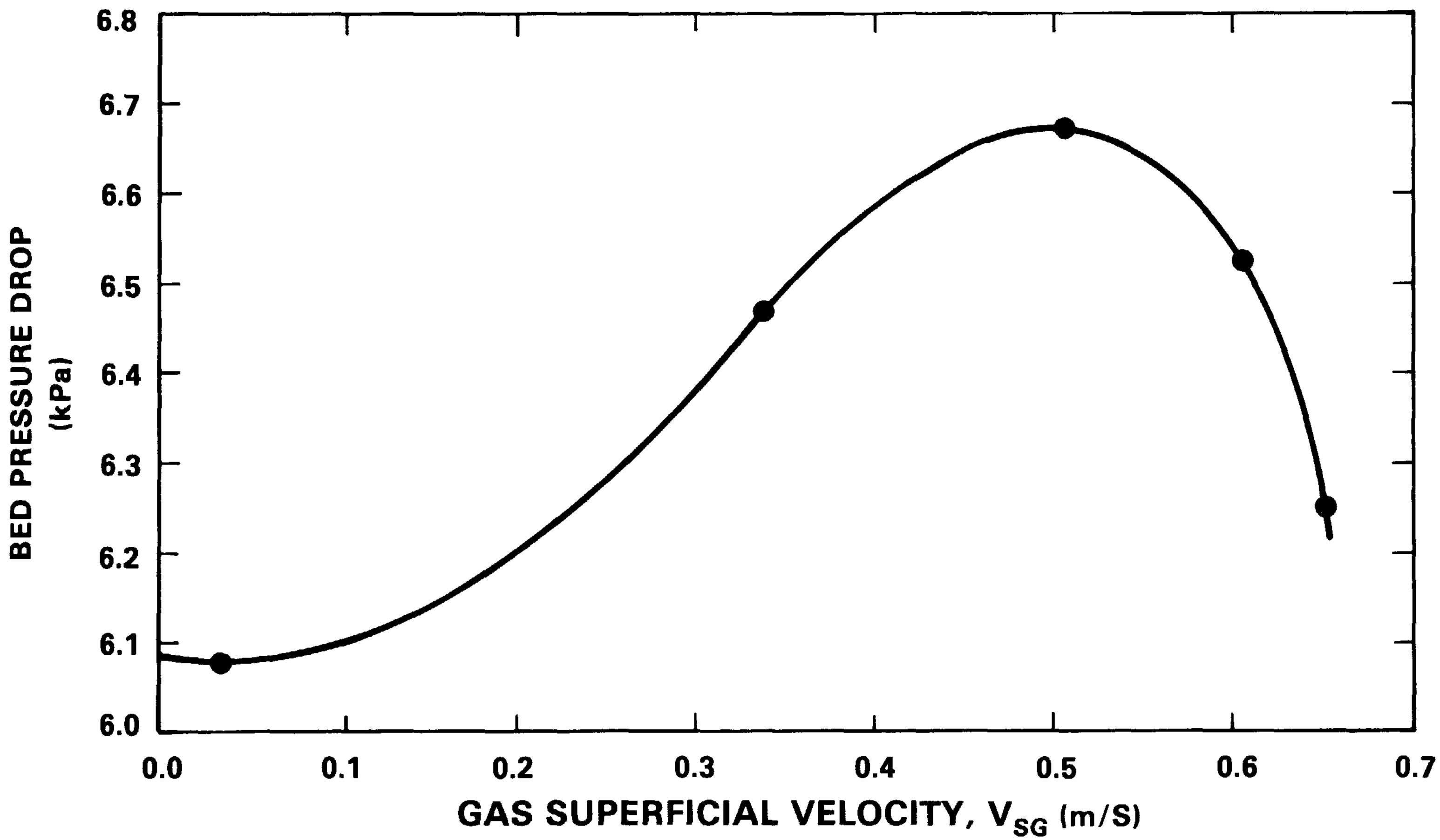

HEDL 8007-104.35

Figure 3. Effect of Gas Velocity on SGS Pressure Drop.

Hydraulic Circulation

The superficial liquid velocity exhibits a maximum as the gas superficial velocity is increased as shown in Figure 4. The induced hydraulic circulation rate is related to the oscillating gas layer and the rate measured is averaged over time. Increasing the bed depth and decreasing the packing diameter increases the hydraulic resistance and decreases the superficial liquid velocity.

The superficial liquid velocity decreases as the liquid level is lowered. For the base bed configuration the minimum liquid level at which water was circulated was 24 cm below the top of the bed at superficial gas velocities between 0.17 m/s and 0.51 m/s. The circulation rate was half the maximum at a liquid level 14-cm below the top support.

Aerosol Penetration

A summary of the efficiency test results is given in Table III. The overall efficiencies were calculated from the mass of aerosol collected within the scrubber liquid and the mass collected on the backup HEPA filter. The average efficiencies were determined from aerosol samples taken from the inlet and outlet ducts. The values shown are for the SGS; values in parenthesis are for the overall system.

The base SGS configuration was a bed 0.610-m long consisting of (+) 0.95 cm to (-) 1.27 cm rock. The HEFD unit was combined with the SGS for tests 6 and 7. A commercial metal demister pad, manufactured by York*, was substituted for the HEFD for test 8.

Efficiencies calculated from aerosol sampling matched reasonably well with those calculated from collected mass. Reducing the bed height by a factor of two increased the SGS aerosol penetration by a factor of seven. The size of packing did not have a measurable effect on aerosol penetration for the size range investigated. The type of aerosol did not affect the scrubber performance.

Combination of the SGS and HEFD resulted in two orders of magnitude reduction in aerosol penetration in test 6. A leaky seal resulted in degraded HEFD performance in test 7, but the aerosol penetration with the HEFD was still an order of magnitude lower than tests without the HEFD. The metal demister pad was not effective in removing aerosols that penetrate the SGS (see results for test 8 in Table III).

During each test run, gas velocity was varied to determine whether removal efficiency varied with flow rate. Efficiencies based on gas samples showed that an overall penetration of approximately 10^{-4} was obtained, independent of the gas flow rate. The SGS thus has an unlimited gas flow turn-down ratio, an important characteristic for containment venting applications.

* Otto H. York Co., Inc., Fairfield NJ, P/N 6W6LTK-304G-QRW304

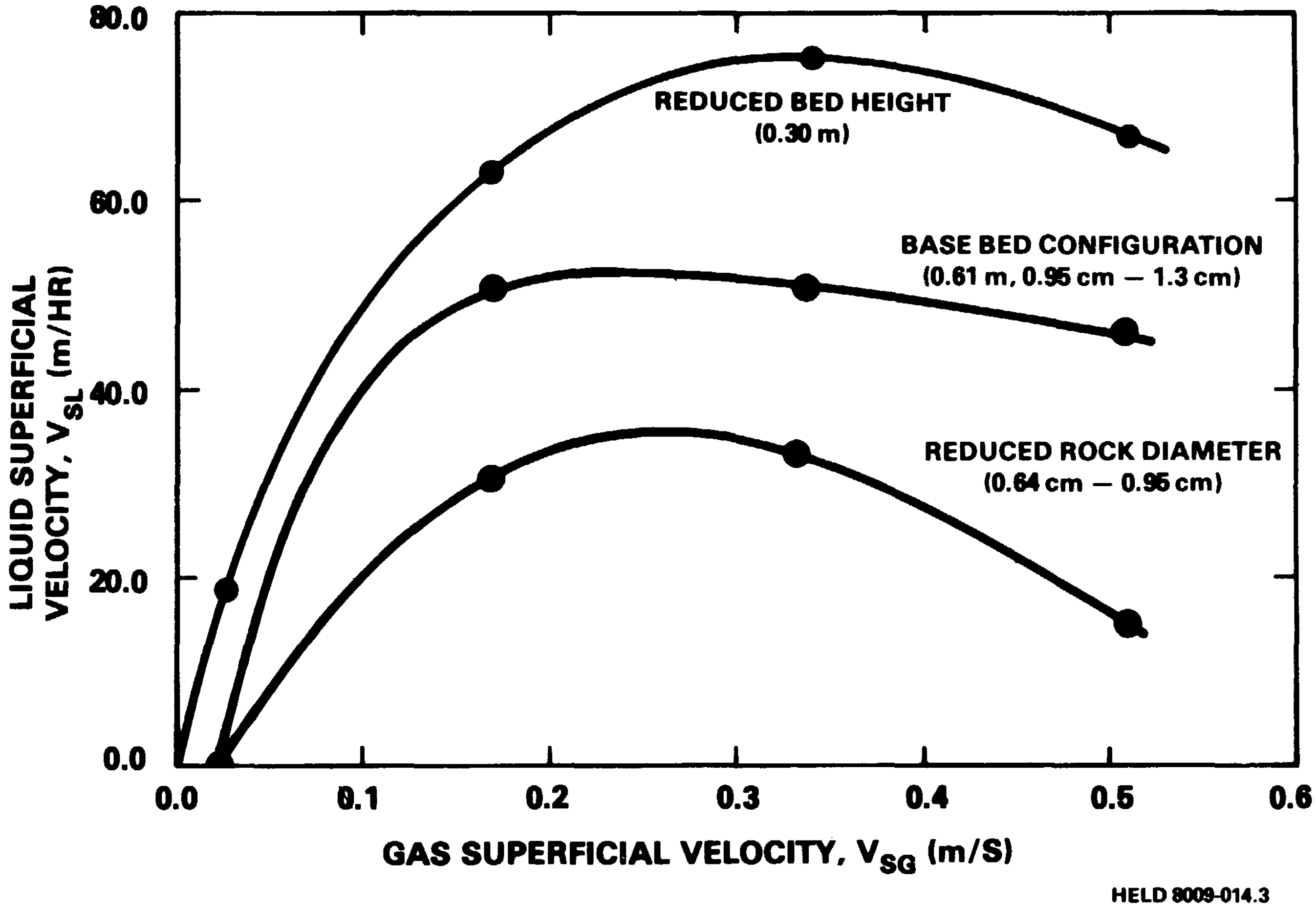

Figure 4. SGS Hydraulic Circulation.

TABLE III. Efficiency Test Results

Test	Overall Efficiency (a)	Average Efficiency (b)	Na Mass Collected, grams	Parameter Tested (c)
1	99.8	99.18	748	Type of aerosol
2	99.8	99.97	590	Type of aerosol
3	98.6	98.78	401	Reduced bed height (0.305m)
4	99.8	99.97	566	Reduced size of packing (0.64 - 0.95 cm)
5	99.8	99.64	106 (Li)	Type of aerosol
6	(99.996)	99.70 (99.998)	4517	Fiber element added (d)
7	(99.97)	99.74 (99.97)	8983	Fiber element added, packing size (1.11 - 1.59 cm)
8	(99.55)	99.76 (99.76)	3007	S.S. demister pad (e)

(a) Determined by mass collected in scrubber solution and on a final HEPA filter.

(b) Determined from aerosol samples taken from the inlet and outlet ducts.

(c) The base bed design was a bed, .305 m in diameter and .610 m in height, consisting of crushed (+ .95 cm to -1.27 cm) basalt rock.

(d) Values in parenthesis are for the scrubber and fiber element combination.

(e) Value in parenthesis is for the scrubber and demister pad combination.

Figure 5 shows a typical result of impactors taken from the inlet duct of the SGS. Log-normal size distributions were assumed and the aerodynamic mass median diameter and geometric standard deviation were calculated from the sodium mass deposited on each stage.

Gas Cooling

Hot gas is cooled as it passes through the SGS by evaporative cooling. The gas leaving the SGS is saturated and cooled to within 2°C of the liquid temperature. Figure 6 shows the gas inlet and outlet temperatures and the liquid temperature as a function of time for test 8.

IV. Discussion

The low aerosol penetration through the SGS indicates that additional removal mechanisms other than inertial forces are important. A model developed by Jackson and Calvert assumes the bed can be represented by a series of semicircular channels.(4) Aerosol particles are assumed to be collected on the channel walls by centrifugal force. The model predicts aerosol penetrations one to two orders of magnitude greater than observed. Additional collection mechanisms, such as flux/force condensation, particle growth, and turbulent agglomeration, undoubtedly make an unaccounted for, but important, contribution to aerosol removal. Definition of the collection mechanisms is an area requiring further theoretical and developmental work.

The hydraulic performance of the SGS was defined for various bed configurations. The hydraulic characteristics agree reasonably well with the results of a study made on a two-phase cocurrent flow in a vertical packed bed.(5)

Scaling the SGS unit to handle high gas flows may be based on a maximum superficial gas velocity of 0.50 m/s. The major uncertainty in scaling the scrubber is the effect of increasing bed diameter on gas distribution. A test bed was built representing a 50 degree sector of a 3.1-m diameter bed sized for 3.1 m^3/s. Figure 7 is a photograph of the sector operating at a superficial gas velocity of 0.50 m/s. The gas distribution was judged acceptable showing that the circular configuration can be scaled up to diameters of at least 3.1 m.

The mass of aerosol that can be removed by the scrubber is determined by the pool volume and a limiting liquid concentration. A reasonable liquid concentration based on solubility limits and viscosity considerations is 5 M NaOH.

The pressure drop across the SGS/HEFD is higher than some alternative scrubbers. However, the excellent performance over a wide range of gas flowrates, the large mass loading, and the high reliability of the system warrant consideration of the SGS/HEFD for other air cleaning problems. Possible applications in the nuclear industry include reprocessing plant offgas treatment, liquid metal research facilities, nuclear waste incinerators, and waste vitrification off-gas treatment.

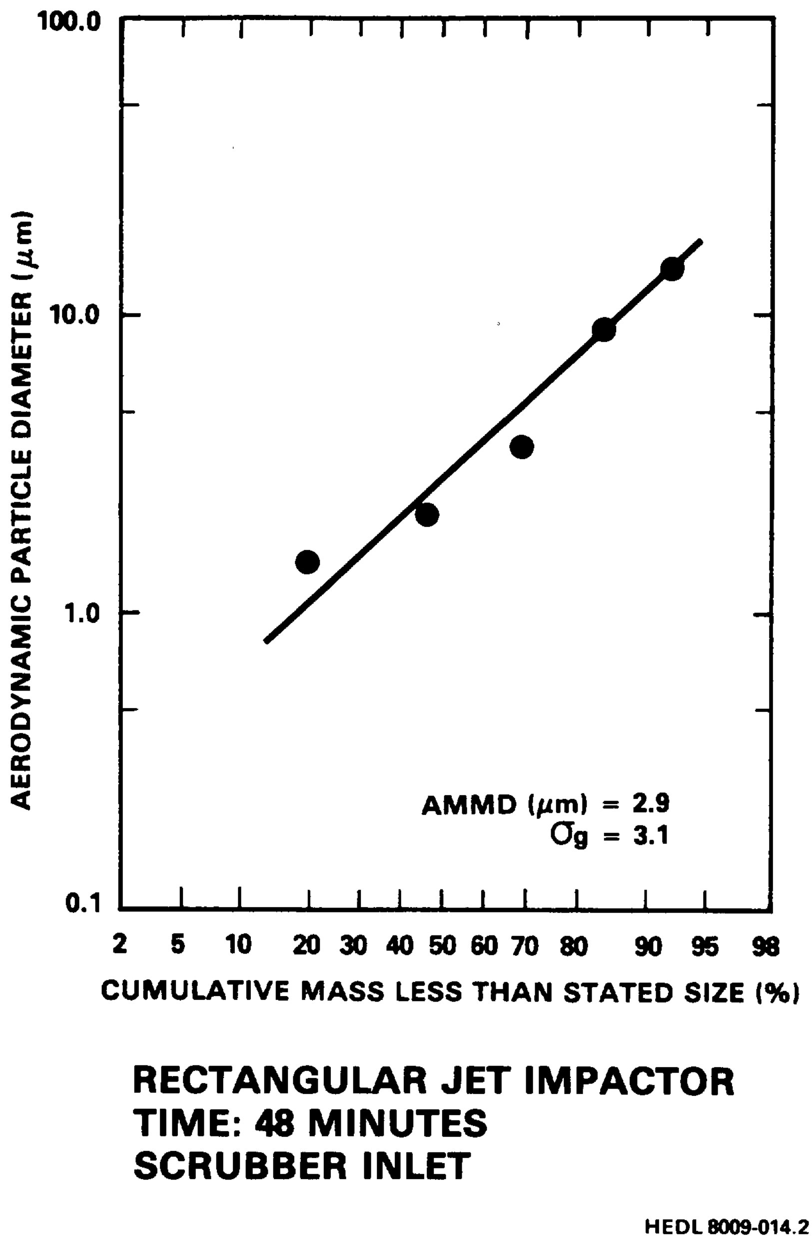

Figure 5. Size Distribution of Inlet Aerosol.

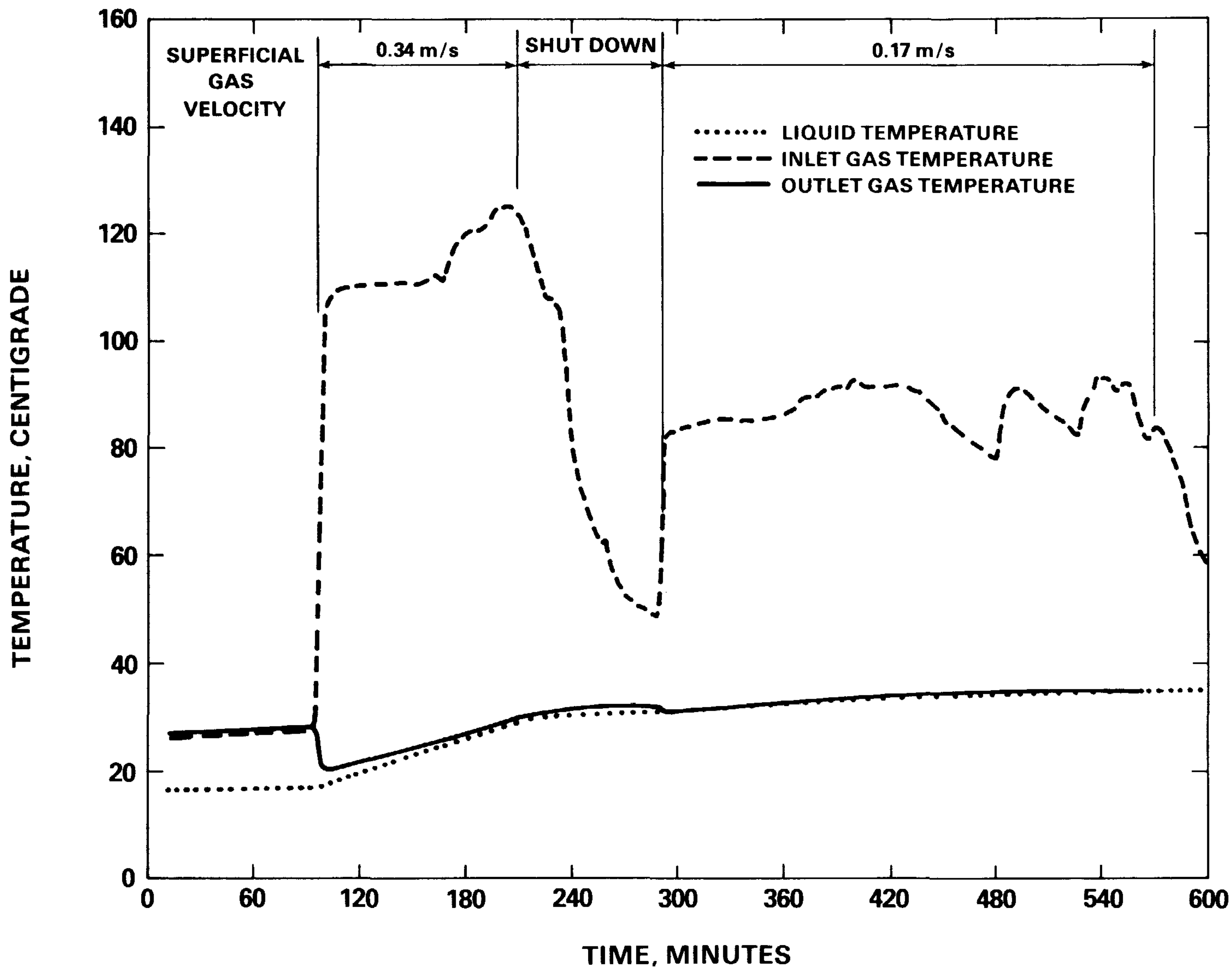

Figure 6. Gas Cooling by the SGS.

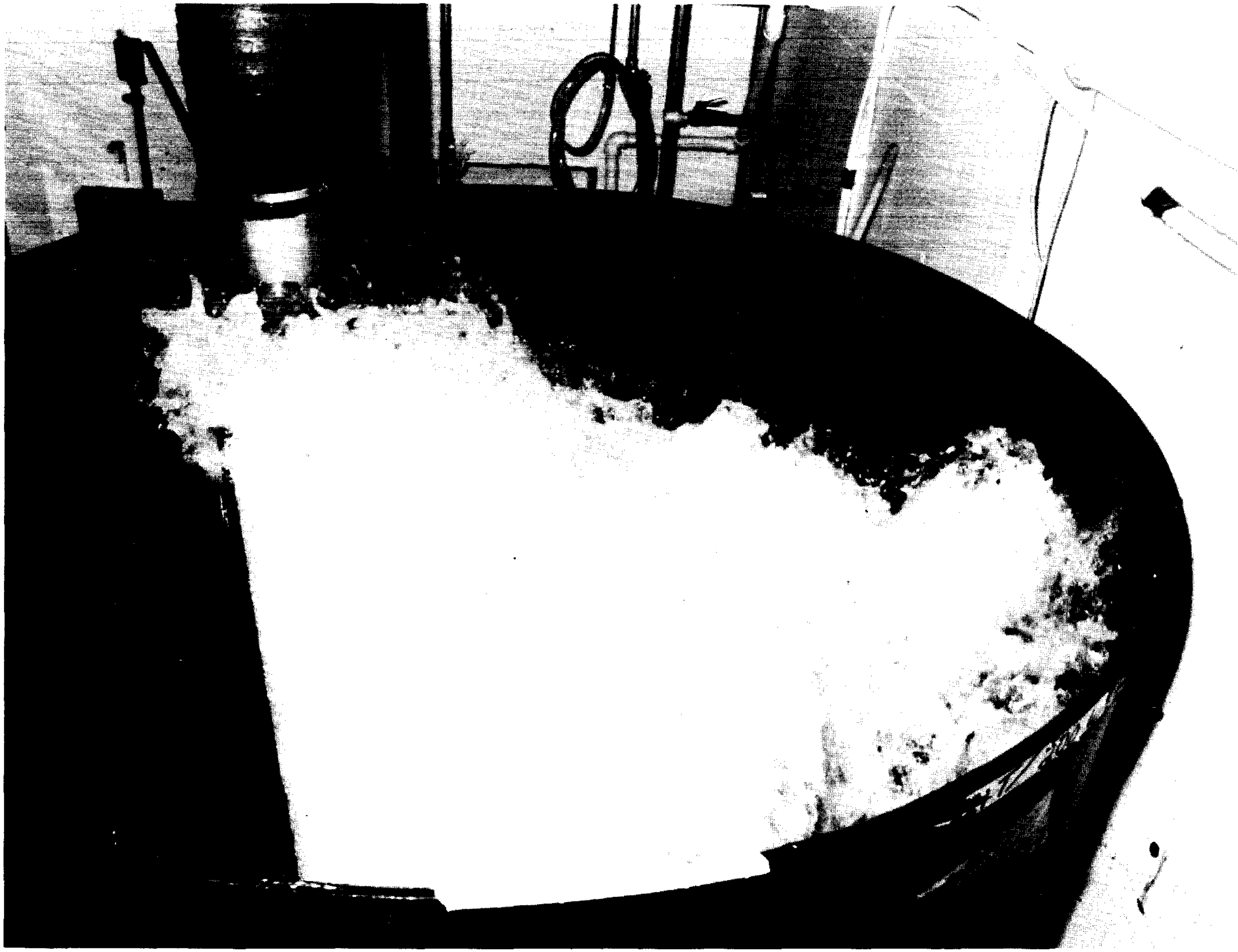

Figure 7. View of upper surface of an SGS designed for 0.47 m^3/sec air flow.

Future work is focused on demonstration testing a unit capable of processing 0.47 m^3/s. The unit will be challanged by various sodium aerosols in four separate tests. Additional work will be performed on evaluating the SGS performance using sodium aerosols at concentrations up to 100 g aerosol/m^3 at gas temperatures up to 650°C. An effort will be made to determine aerosol penetration through the SGS as a function of particle size.

V. Summary and Conclusions

The test series demonstrated that the SGS/HEFD concept is a viable system for removing aerosols from vented and purged containment atmospheres under conditions postulated for severe LMFBR accidents. A series of eight tests was performed using sodium and lithium aerosols. The aerosol test experience sums to 75 hours of operation, approximately 6400 std m^3 of cleaned gas at inlet gas temperatures up to 125°C, and 33 kg of collected aerosol. Specific conclusions are:

- An acceptable bed design configuration is a bed 0.61-m deep composed of 0.95-cm to 1.27-cm crushed rock.
- An appropriate design gas superficial velocity is 0.5-m/s. Scrubber performance is maintained to gas velocities below 0.03 m/s.
- A novel feature of the SGS is gas-induced liquid circulation through the bed. The liquid circulates at superficial velocities up to 60 m/hr.
- The scrubber pressure drop is essentially equivalent to the static head of water, or 6.7 kPa for a 0.61 m deep bed.
- The aerosol removal efficiency for sodium aerosols through the SGS was measured to be 99.8%. The SGS/HEFD system aerosol removal efficiency exceeded 99.99%.
- Removal efficiency was essentially the same for three chemical forms of sodium aerosol and lithium aerosol.
- The total mass loading of the system is dependent on the liquid pool volume and a limiting concentration level. A limit of 5 M-NaOH is recommended based on solubility and viscosity considerations.

VI. References

1. R. K. Hilliard, J. D. McCormack, and A. K. Postma, "Evaluation of Air Cleaning System Concepts for Emergency Use in LMFBR Plants," HEDL-TME 76-41, Hanford Engineering Development Laboratory, Richland, Washington (1976).

2. R. K. Hilliard, et.al., "Containment Air Cleaning for LMFBRs," in Proc. of the International Meeting on Fast Reactor Safety Technology, Seattle, Washington, Am. Nucl. Soc., August 19-23, 1979.

3. J. D. McCormack, R. K. Hilliard, and A. K. Postma, "Large-Scale Tests of Aqueous Scrubber Systems for LMFBR Vented Containments," HEDL-SA-2121 FP, Paper 5-4, presented at 16th DOE Nuclear Air Cleaning Conference, October 20-23, 1980, San Diego, California.

4. S. Jackson, S. Calvert, "Entrained Particle Collection in Packed Beds," AIChE Journal 12, 1075-1078, November 1966.

5. J. L. Turpin, R. L. Huntington, "Prediction of Pressure Drop for Two-Phase, Two-Component Concurrent Flow in Packed Beds," AIChE Journal 13, 1196-1202, November 1967.

DISCUSSION

CARNES: We operate the Hot Fuel Examination Facility in Idaho Falls. One of the problems that we are concerned about would be a sodium fire in an inert examination cell. Are there any other fluids that you could use for scrubbing in this gravel bed that would serve the same purpose?

OWEN: On a much, much smaller scale, I have looked at the use of silicone fluids, heat transfer fluids like Mobiltherm. I have not investigated whether sodium aerosol remains in the fluid, but I see no reason why that might not be a viable way to go.

ROUYER: The facility you have designed is for three cubic meters per second?

OWEN: Yes.

ROUYER: So, the size of the entrance, the area, would be 6 square meters?

OWEN: Right.

ROUYER: I would like to have an idea of the dimensions.

OWEN: For a 3 cubic meter per second unit?

ROUYER: Yes. I wonder which type of accident we are dealing with, because for some accidents in reactors, the size will be dimensioned by the heat to be absorbed.

OWEN: The way I would design the bed is to use a superficial gas velocity of 0.51 meters per second and base the surface area of the bed according to that. The depth would be 0.609 meters. Then, the tank volume can be sized either to take care of solubility or to take care of the heat load. It depends whether or not you are going to allow additional water to be put into the tank during the accident.

DESIGN CRITERIA AND CONCEPTS FOR VENTED CONTAINMENT SYSTEMS*

H. C. Walling and A. S. Benjamin
Sandia National Laboratory
Albuquerque, New Mexico

P. Cybulskis
Battelle Columbus Laboratories
Columbus, Ohio

Abstract

Vented containment systems are commonly considered to be effective in reducing the consequences of severe accidents in light water reactors. The principal function of venting is to prevent uncontrolled failure of the reactor containment building should its integrity be challenged by the physical conditions generated during an accident. In so doing, radioactive material can be filtered from the vented gases to reduce the environmental impact. This presentation summarizes results of research concerning potential design requirements of such systems. Findings related to air cleaning are emphasized.

Accident sequences from WASH-1400 were selected and analyzed with the MARCH/CORRAL code to provide an envelope of design conditions. The time-dependent pressures and temperatures in containment were calculated as were the concentrations of steam, non-condensible gases and airborne fission products in the containment atmosphere. The phenomenon found to be most challenging to containment integrity was a pressure spike resulting from rapid steam generation and/or hydrogen burning. The peak pressures in some sequences exceed the likely failure pressure.

Conceptual designs were developed for preserving containment integrity. These include containment pressure relief or depressurization with various venting rates. Anticipatory venting, venting to the atmosphere, venting to a separate building, and venting followed by recirculation back into containment are considered. The effects of these schemes on the important system parameters were identified. The advantages and disadvantages of alternative schemes and their implications for the design of filtration equipment are discussed.

For each venting strategy several levels of filtering effectiveness were considered. The simplest option

*This work funded by U.S. Nuclear Regulatory Commission.

developed is a once-through gravel-filled suppression pool. More sophisticated options involved sand filters, molecular sieves, charcoal adsorbers and HEPA filters. Results of accident consequence calculations using the CRAC code indicate the relatively simple options can provide substantial reductions in consequences of certain accident sequences.

Introduction

Safety research for light water reactors (LWRs) in the U.S. is increasingly focusing upon severe accidents in which core melting may occur. The primary focus of this research is on prevention rather than mitigation, however, some research has been directed toward the development and analysis of systems that mitigate severe accidents in the unlikely event that the engineered safety features (ESFs) fail.

The current interest in filtered-vented containment systems (FVCSs) in the U.S. stems from the Reactor Safety Study (RSS).[1] The RSS determined that containment failure due to overpressurization represents the largest contributor to reactor risks. Subsequent studies [2-5] have reinforced the idea that containment venting could reduce reactor risk by reducing the probability of containment overpressurization. In April 1979, the USNRC initiated a program at Sandia National Laboratories to investigate filtered-vented containment concepts for light water reactors. That program has the following features:

1. Development of conceptual designs of vent-filter systems which have the potential to mitigate the effects of accidents (particularly core melt accidents) that are beyond the current design basis.

2. Determination of the potential reduction in radioactive releases for core-melt accidents and the resultant reduction in overall risks.

3. Determination of the effect of the vent-filter on non-core-melt accidents and on normal operations.

4. Specification of system performance and safety design requirements for vent-filter systems.

5. Quantitative analysis of values versus impacts.

Sandia's work on filtered-vented containment system design, development and evaluation during the first year of the program are described in Ref. (6) - (8). This paper summarizes that work and discusses the work in progress. The contents of this paper include a description of the baseline pressurized (PWR) and boiling water reactors (BWR) analyzed to date, a summary of key accident scenarios and feasible venting strategies to mitigate them and a discussion of filtered-vented containment design options. Emphasis is placed on the air cleaning aspects of such design options.

Baseline Reactors

The NRC sponsored Sandia study includes an investigation of filtered-vented containment system design concepts for the following primary containment types: (1) large-dry pressurized water reactor (PWR) containment, (2) Mark I boiling water reactor (BWR) containment, (3) ice condenser PWR containment and (4) Mark III PWR containment. Preliminary analysis for category (1) and (2) above have been performed. Some characteristics of the large-dry PWR containment and the Mark I BWR containment are presented in Table I.

Table I Characteristics of the Baseline Reactors

Reactor	PWR	BWR
Thermal Power	3025 MW	3293 MW
Containment	Steel-lined, reinforced concrete domed cylinder	Mark I drywell/wetwell, inerted to less than 5% O_2 (molar)
Containment Cooling	(1) Containment air coolers, 112 MW max. (2) Containment sprays, 20,000 ℓ/min max.	Suppression pool circulated through heat exchanger cooled by HPSW. 82 MW max. cooling
ECC Water Sources	(1) 4 accumulators pressurized to 45 bar (abs), 7.9×10^4 ℓ. (2) RWST, 1.3×10^6 ℓ.	(1) Suppression pool, 3.9×10^6 ℓ (2) CST, 5.7×10^5 ℓ.
High Pressure ECC	HPI system, injects from RWST, 4700 ℓ/min max.	HPCI system, powered by reactor steam, injects from CST or suppression pool, 19,000 ℓ/min max. Can be supplemented by RCIC.
Low Pressure ECC	LPI system, injects from RWST, recirculates from recirculation sump, 23,000 ℓ/min max.	(1) LPCI system, injects and recirculates from suppression pool, 1.5×10^5 ℓ/min max. cross tie with HPSW system allows injection of river water into reactor vessel. Some water can be diverted to containment sprays. (2) CSI system, injects from CST or suppression pool, recirculates from suppresion pool, 47,000 ℓ/min max.
Primary System Depressurization	Manual, through S/R valves. Requires ac power.	ADS. Requires dc power.

Accident Scenarios and Venting Strategies

In order to investigate design options for the filtered-vented containment system it was necessary to consider a variety of accident scenarios similar to those considered in the Reactor Safety Study (RSS). The accidents selected for study represent best estimates of those accidents from the RSS that dominate risk to the public for each reactor containment type. Also included are accidents that may not dominate risk but provide an unusual challenge to the filtered-vented containment system. Analysis of each accident scenario provided the basis for selecting design options/venting strategies capable of mitigating the effects of the accident.

PWR Accident Scenarios

A brief description of the accident scenarios selected from RSS for application to the PWR containment is given in Table II.

Table II PWR Accident Scenarios

RSS Accident Notation	PWR Accident Sequences	Estimated Contribution to Reactor Risk
TMLB'	Loss of offsite and onsite ac power for at least 3 hours.	High
	Failure of power conversion system and auxiliary feedwater system.	
S_2D	Small LOCA with failure of ECC injection and recirculation.	High
S_2G	Small LOCA with failure of containment heat removal.	Moderate
AB	Large LOCA with loss of offsite and onsite ac power.	Small

Calculations of containment pressure vs. time were made for the four listed accidents using the MARCH computer code.[9] The results of those calculations are presented in Figure 1.

The calculations indicate that a large pressure spike could occur if melt-through of the reactor vessel were to happen. The cause of the containment pressure spike varies, but combinations of the following are responsible:

1. Steam release from the primary system to the containment when the reactor vessel fails at high pressure (accidents TMLB' and S_2D).

2. Rapid steam formation caused by molten core interaction with water existing in the cavity at the time of reactor vessel failure (accident AB).

3. Rapid steam formation caused by flashing of some of the residual water in the primary loops when the reactor vessel fails, and by dumping of the remainder of this residual water onto the molten core in the cavity (accidents TMLB' and S_2D).

4. Rapid steam formation caused by discharge of accumulator water at the time of reactor vessel failure and interaction of this water with the molten core in the cavity (accidents TMLB' and S_2D).

5. Deflagration of the hydrogen produced by Zircaloy-steam reaction, triggered by the interaction of the molten core with the concrete in the cavity (accidents AB and S_2D).

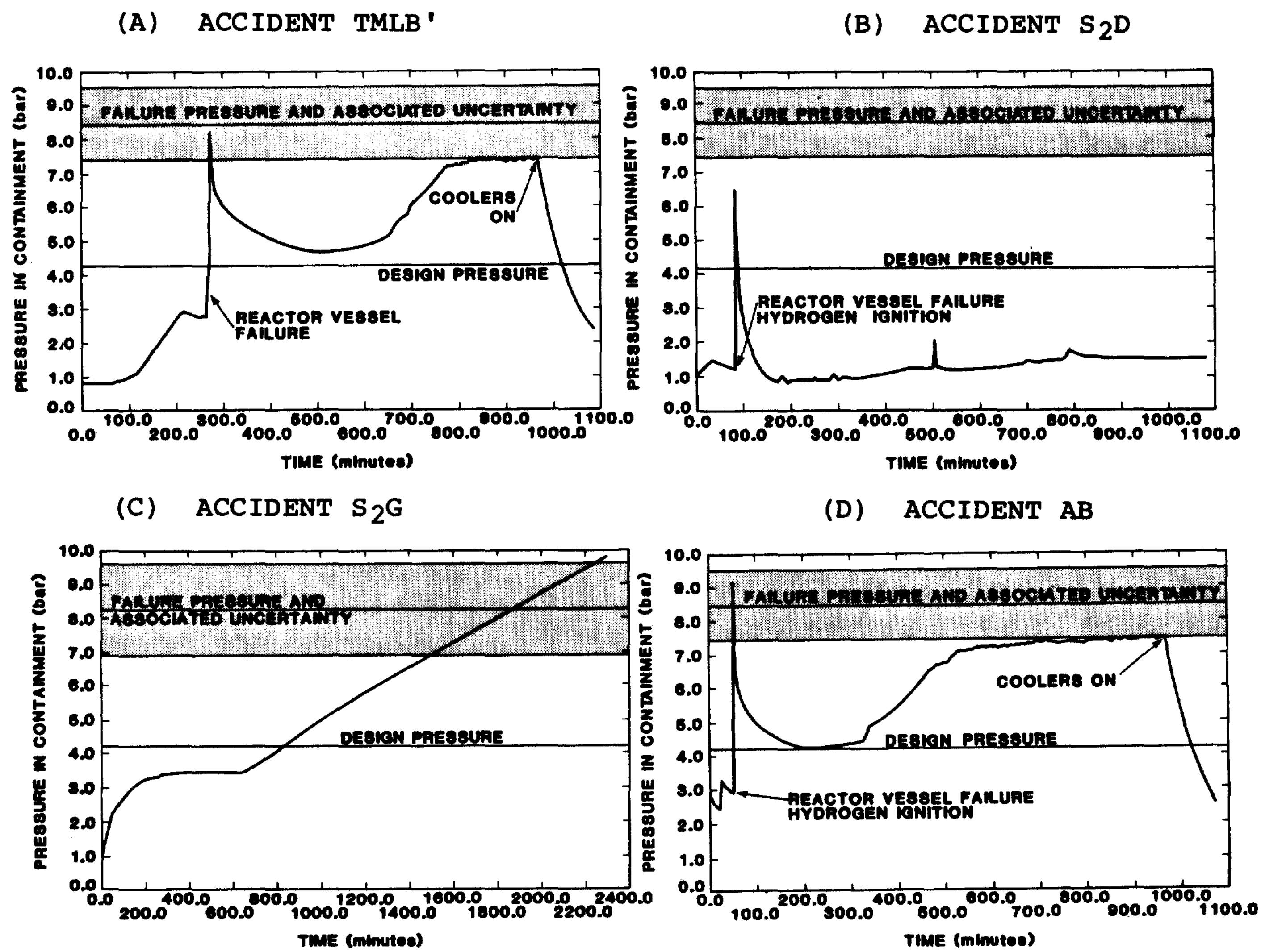

Figure 1 MARCH Code Calculations of Containment Pressure Versus Time for Four Hypothesized Accidents in the Baseline PWR Plant

The magnitude and duration of the spike are subject to assumptions regarding the nature of core material interactions with water which may prove to be conservative. Experiments will be performed soon to investigate the phenomenology of steam spikes.

PWR Vent Strategy 1. In this strategy, containment internal pressure is vented at a low flow rate (400 m^3/min) when the containment pressure exceeds 6 bar. When the internal pressure falls below 6 bar the control valve would close. In this way the containment internal pressure would be maintained at or below the containment design pressure. The advantages of this strategy are its simplicity and the minimum potential for adverse effects on engineered safety features (ESFs).

PWR Vent Strategy 2. Deliberate depressurization of the primary loop after most of the water has boiled off could be helpful during accidents initiated by transients or during small break loss of coolant accidents (LOCAs). Deliberate depressurization of the reactor primary loop would require either automatic controls or operator judgement. This vent strategy has the disadvantage that an actuation error could cause a LOCA that otherwise would not have happened.

PWR Vent Strategy 3. Anticipatory containment depressurization could prevent containment overpressurization by forecasting a core melt and venting containment in advance. During the interval between initiation of core melt and failure of the reactor vessel lower head there is time to reduce containment internal pressure to a level where subsequent pressure spikes would not exceed the containment failure pressure. Anticipatory venting could also reduce the magnitude of a hydrogen burn by removing hydrogen and oxygen from the containment.

Parameters used to initiate anticipatory venting might be sustained low reactor vessel water level, high containment radiation levels, high reactor vessel temperature and high containment internal pressure. In order to prevent the possibility of emergency core cooling (ECC) failure due to recirculation pump cavitation it might be necessary to place a booster pump into the ECC recirculation inlet to meet the net positive suction head (NPSH) requirements of the ECC recirculation pump. It would also be necessary to install vacuum breakers into the present containment boundary and to limit containment spray operation in order to counteract the possibility of a severe containment vacuum.

Anticipatory containment venting introduces greater potential for unnecessary radioactive release than other strategies because some accidents with incipient core melt might not threaten containment integrity. The anticipatory containment vent parameters (high radiation levels, high reactor pressure and temperature and low reactor water) might indicate incipient core melt, such as at Three Mile Island, and might signal the containment vent to open, whereas a full-scale core melting may not develop and no threat to the containment may occur. However it is felt that the magnitude of such unnecessary radioactivity releases via the filtered-vented containment system would be small compared with uncontrolled release via a ruptured containment.

Figure 2 shows the effect on containment pressure vs. time of implementing PWR vent strategy 2 and 3 on the TMLB' accident. It can be seen that the peak pressure is reduced below the containment failure pressure.

(A) PWR VENT STRATEGY 2

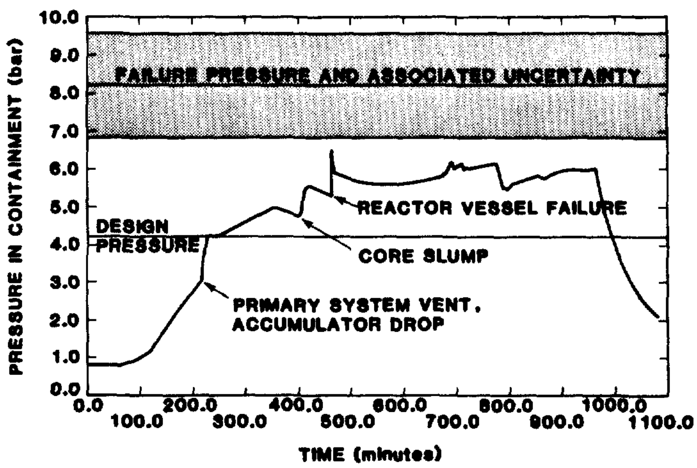

(B) PWR VENT STRATEGY 3

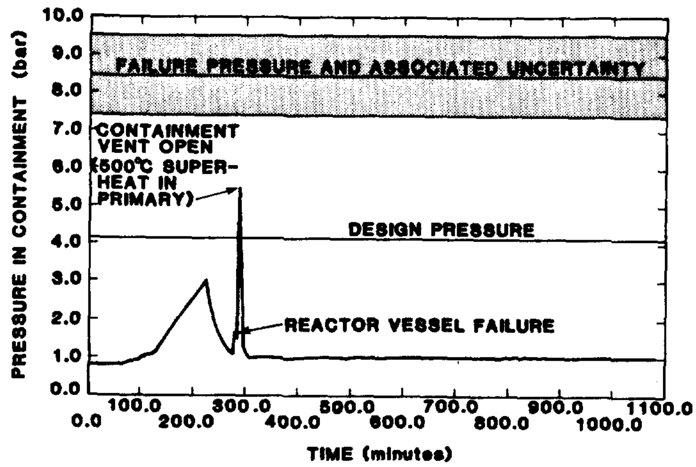

Figure 2 MARCH Code Calculations of Containment Pressure Versus Time for the Accident TMLB' in the Baseline PWR with Different Venting Strategies

BWR Accident Scenarios

Four accidents were selected from the RSS as posing moderate to high risk to the public should the primary containment fail. Those four accidents are described in Table III.

Table III BWR Accident Scenarios

RSS Accident Notation	BWR Accident Sequences	Risk
TW	Transient initiating event with failure of suppression pool cooling.	High
TC	Transient initiating event with failure of reactor protection system.	High
TQUV	Transient initiating event with failure of feedwater and ECC availability.	Moderate
AE	Large LOCA with failure of ECC injection.	Moderate

The risk dominating accident sequences in the BWR (TC and TW) lead to primary containment overpressurization while the core is partially covered with water and hence not melted. Thus a primary requirement of the BWR filtered-vented containment system would be the prevention of containment overpressurization without degradation of the ECC function.

For the accidents TQUV and AE where core meltdown precedes containment overpressure a pressure spike occurs when the reactor vessel fails. The sharp pressure rise is due to:

1. Hydrogen release from the reactor vessel to the containment. This rapid containment pressurization can be prevented by the use of the automatic depressurization system (ADS).

2. Hydrogen formation caused by zirconium-steam reaction when the reactor vessel fails and the molten core falls into water.

Figure 3 presents the pressure vs. time history of the four BWR accidents (TC, TW, TQUV and AE).

BWR Vent Strategy 1. This strategy (low-volume containment pressure relief) is similar to PWR vent strategy 1 and requires approximately the same flow rate (400 m^3/min). Venting from the wetwell allows the suppression pool to be used as a filter for the drywell environment.

This low flow rate option would prevent accidents TW and TQUV from overpressuring containment, but would not be adequate for AE and TC. Operation of this vent strategy during an accident with a failed suppression pool cooling system would result in a reduction of the NPSH below the design basis for the low pressure coolant recirculation (LPCR) pumps. Booster pumps could be incorporated in the LPCR system in order to increase the NPSH and prevent cavitation of the (LPCR) pumps. The LPCR pump inlet could be diverted from the suppression pool to another source (via existing cross-overs) such as the high pressure service water system (HPSW).

<u>BWR Vent Strategy 2</u>. During the TC accident it is possible to continue high pressure coolant injection (HPCI) and prevent a total core meltdown as long as water is available. Containment venting with a mass flow equal to the rate of steam formation (as a result of HPCI) would create a steady flow process into the primary and out to the suppression pool then into the wetwell and out the containment vent.

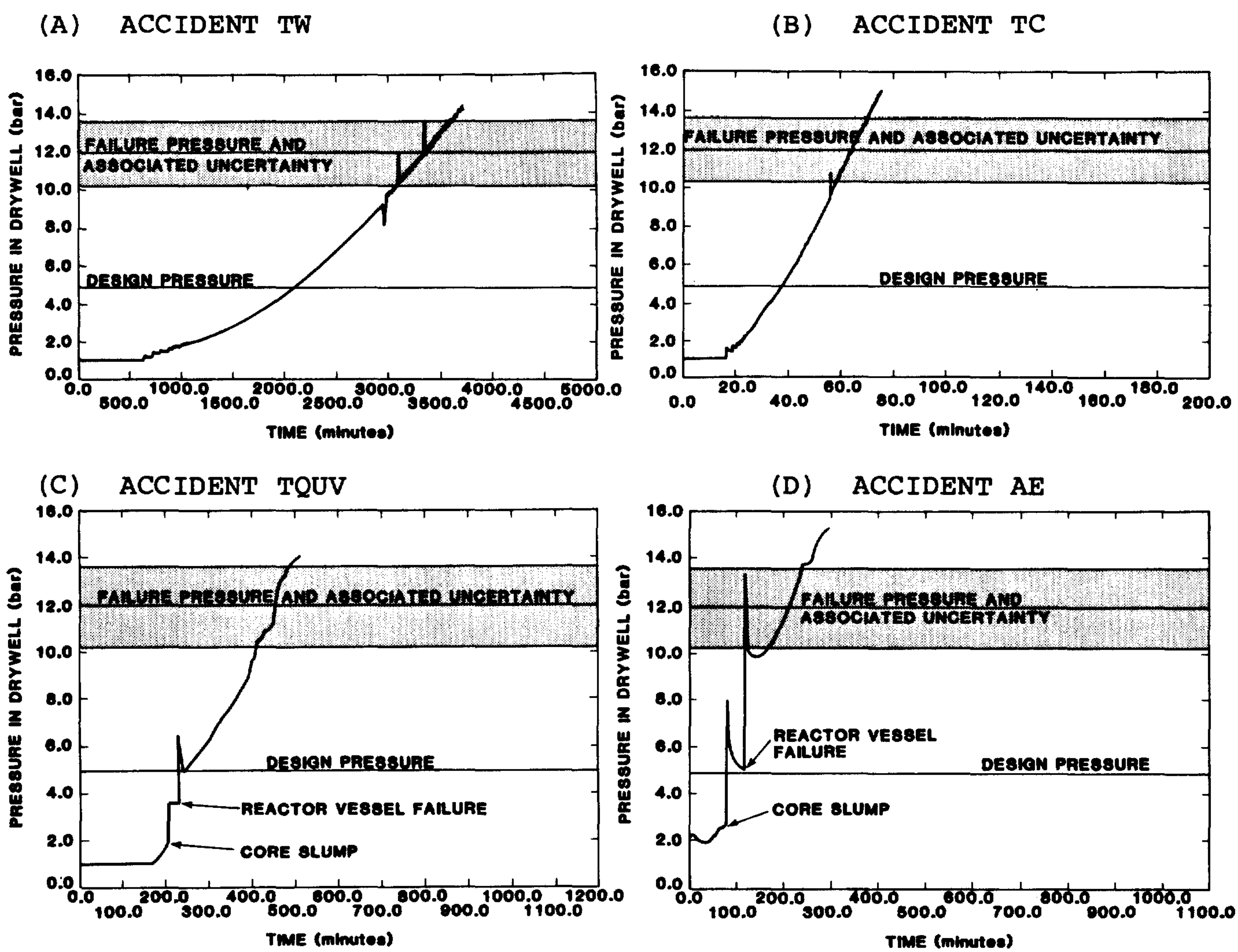

Figure 3 MARCH Code Calculations of Containment Pressure Versus Time for Four Hypothesized Accidents in the Baseline BWR Plant

This steady state situation would be achieved with a vent rate of 4000 m^3/min at a containment internal pressure of 6.8 bar.

Success for this venting strategy during the TC accident depends upon the restoration of the reactor protection system within 3 hours or the availability of an external water source (such as the high pressure service water) to supply the HPCI system indefinitely.

BWR Vent Strategy 3. This strategy (anticipatory venting) is similar to the PWR vent strategy 3. It would be effective in preventing drywell failure due to pressure spikes except when the suppression pool is saturated at the onset of wetwell venting. Suppression pool saturation would slow containment depressurization because of boiling from the pool.

Filtered-Vented Containment System Designs

PWR Design Options

Five filtered, atmospheric vented design options and a filtered, contained design option for the PWR under study were formulated. These options represent successively higher levels of fission product removal from the containment vent gas stream.

PWR vent-filter design option 1 is shown schematically in Figure 4. This is the most simple of all the options in that it consists of a gravel chamber as the only filter component. The gas stream is vented through a valve manifold in an existing penetration in the concrete containment vessel into a vent line of approximately 1.0 m diameter. The filter element

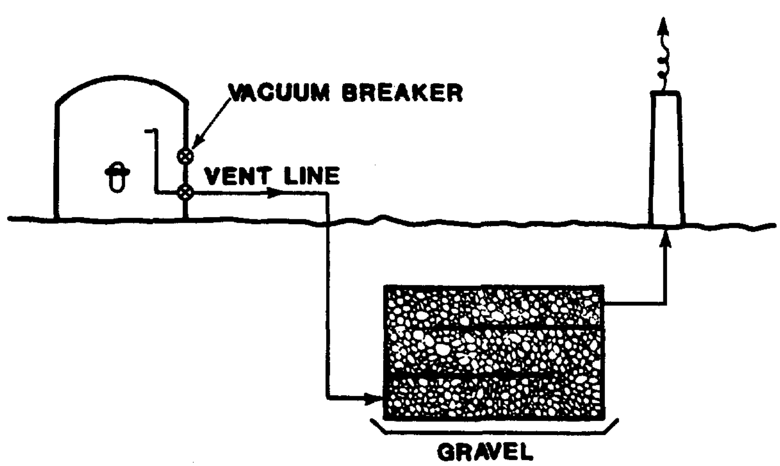

Figure 4 PWR Design Option 1

is a buried gravel bed 20 m long x 10 m deep x 40 m wide for the low flow (400 m^3/min) vent strategy. The dimensions of the bed would be larger to accommodate the vent strategy 3 (2500 m^3/min). The filtered noncondensible gas stream would then discharge to the atmosphere via a tall stack. Recent experiments with crushed gravel suggest that gravel beds of sufficient height will remove submicron particles without excessive pressure drop.[10] The pressure drop across the bed is designed to be less than 0.7 bar.

The advantages of option 1 are its simplicity, low cost, and that it requires no electric power. Disadvantages are the lack of proven performance with large scale systems and an unknown decontamination factor that is sensitive to particle size and gas velocity.

Vent-filter design option 2 is based on a system being developed at Hanford Engineering Development Laboratory.[11] This option is shown in Figure 5 and consists of a gravel bed

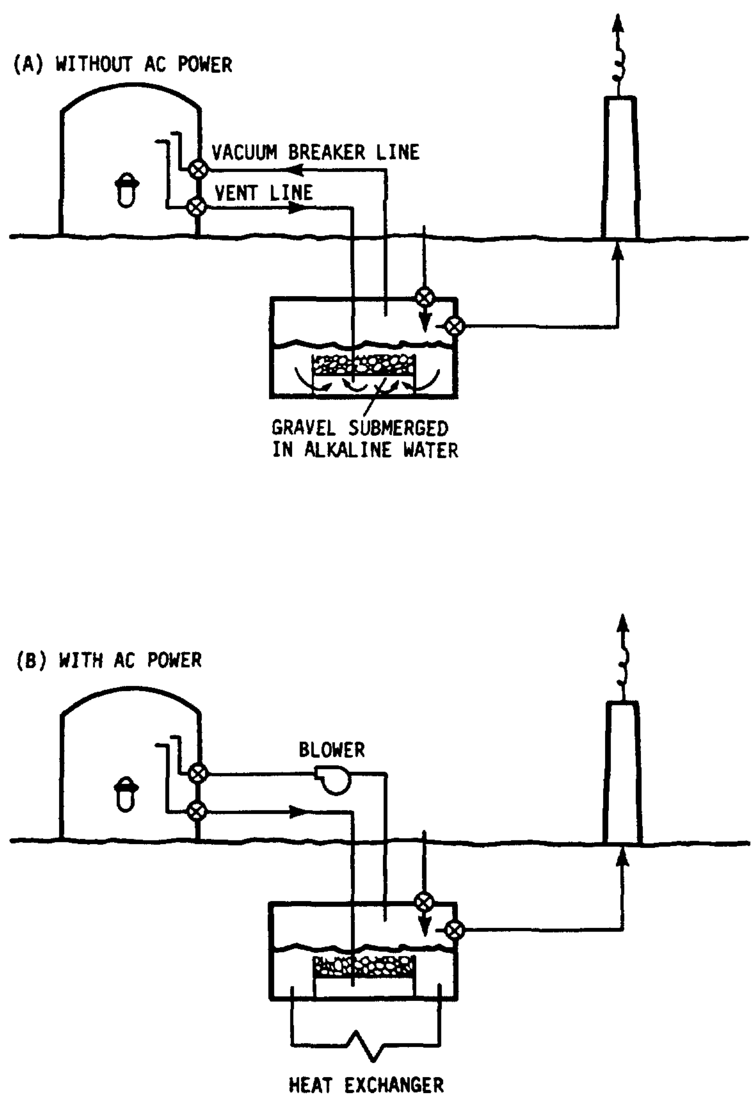

Figure 5 PWR Design Option 2

submerged in an alkaline water pool. This option has the capability to condense steam, which option 1 does not. Estimated fission product removal efficiencies are: 98% particles, 98% I_2, 50% CH_3I, 0% Xe and 0% Kr. In this option a provision for re- circulation of the filtered containment exhaust and long term heat removal from the suppression pool has been made.

Design option 3 is shown schematically in Figure 6 in both the passive and recirculation mode. This option consists of a

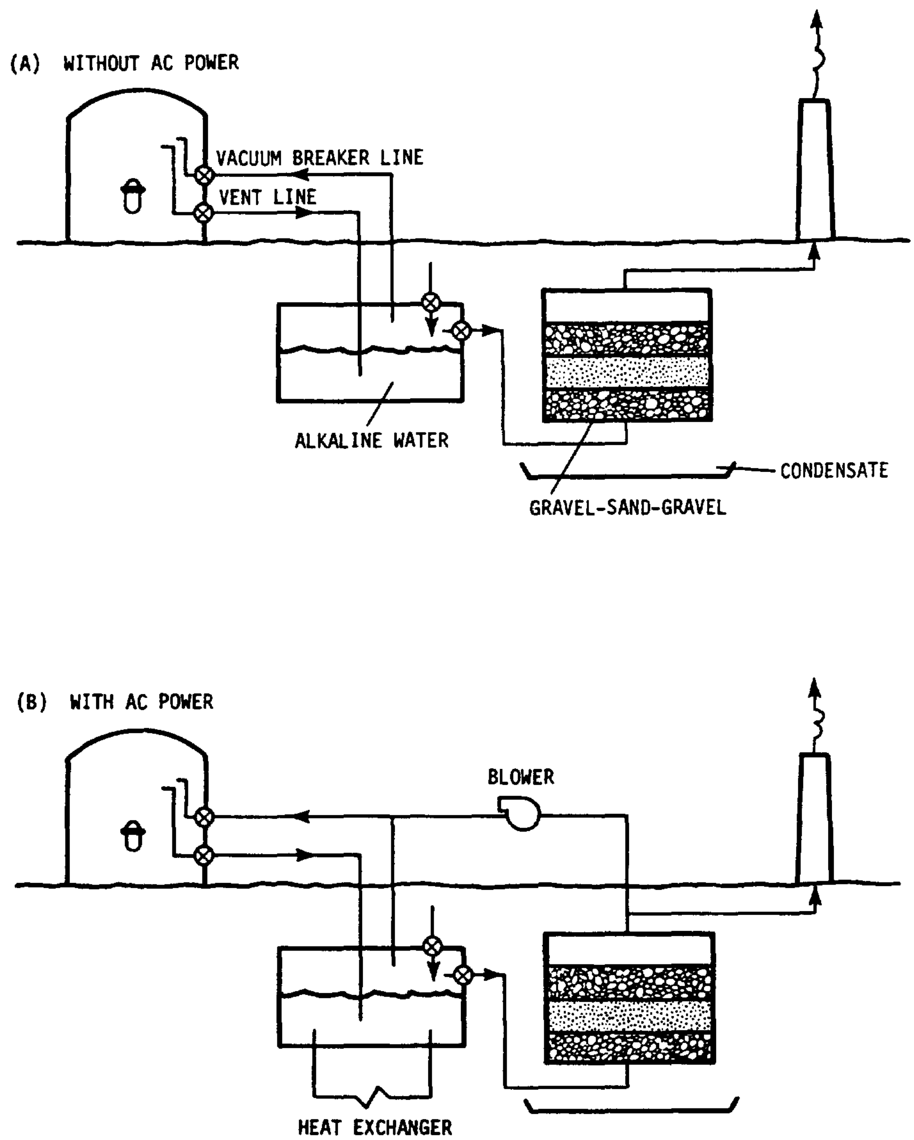

Figure 6 PWR Design Option 3

BWR type suppression pool shown in Figure 7 and a sand-gravel filter shown in Figure 8. Suppression pools are a tested and proven method of cooling and condensing gas streams. Suppression pools require less volume than crushed rock for the same heat load and provide a solution to the long term heat removal via heat exchangers in the wetwell. In this option the toroidal shell has a volume of 8500 m^3 of which 50% is chemically treated water. The 4250 m^3 of water will condense all the steam generated during the TMLB', AB and S_2D accidents. The 4250 m^3 air space allows for the condensate storage. The entire torus and all piping is located below grade in a concrete line pit. In order to maintain a 1.25 m submergence over the downcomer outlets a spillway is located to allow for condensate carryover into the air space. The pressure drop across the suppression pool is designed to be 0.13 bar. This pressure drop should present no problems because the driving pressure (containment internal pressure) will be on the order of 5.0 bar. The piping from containment to the suppression pool would have to be capable of transmitting a peak flow rate

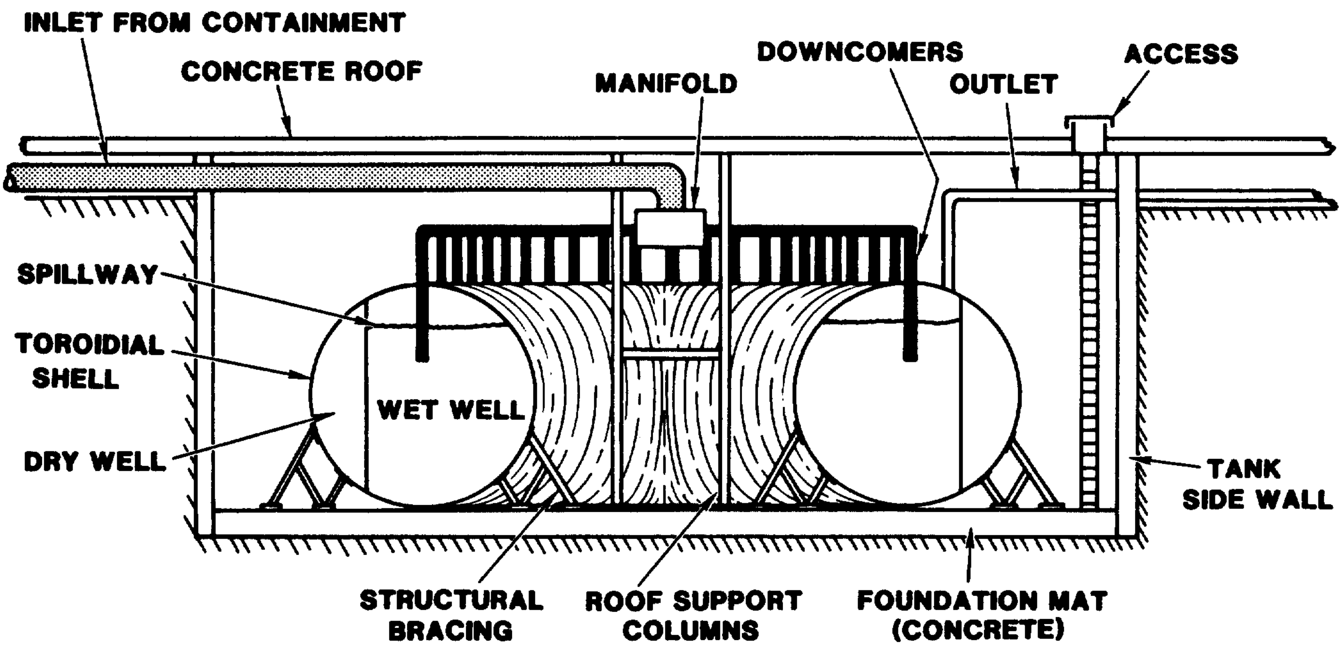

Figure 7 Suppression Pool Section

of 7000 m^3/min and a nominal flow of 1400 m^3/min. The existing purge penetrations would satisfy these requirements.

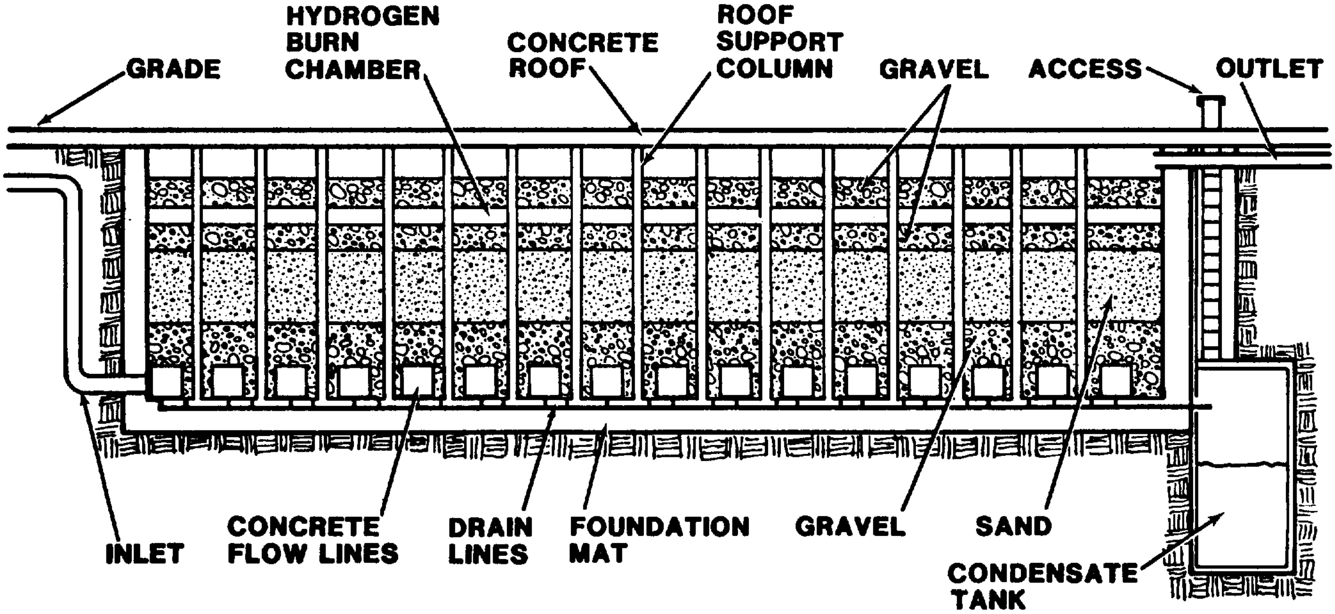

Figure 8 Sand-Gravel Filter Section

The sand-gravel filter shown in Figure 8 consists of a large buried concrete vault filled with alternate layers of gravel and sand. The approximate dimensions of the vault are 36 m long by 36 m wide by 15 m deep. A drain network and integral condensate storage tank are provided to store the contaminated condensate. The structure was designed to handle a flow of 1400 m^3/min at a pressure drop of 0.04 bar maximum. A space is provided in the chamber to accommodate a hydrogen ignition source. The so-called hydrogen burn chamber/space is overlaid by a gravel layer; this layer serves as a flame arrestor and heat sink for the combustion gases. Total fission product removal efficiencies for Option 3 are estimated to be: 99.98% particles, 98% I_2, 50% CH_3I, 0% Xe and 0% kr.

Design option 4 consists of the toroidal suppression pool and sand-gravel filter of option 3 plus a zeolite-charcoal filter downstream from the sand-gravel filter. This option is shown schematically in Figure 9. The zeolite-charcoal filter consists of a wafer shaped tank about .5 m thick and 12 m in diameter. The wafer is fabricated of 304 stainless steel and is gas/water tight. The water is filled with a top layer of 10 cm layer of triethylenediamine (TEDA) impregnated charcoal. These two layers are followed by a layer of HEPA filters to trap charcoal and other particulate. The layers of filter media

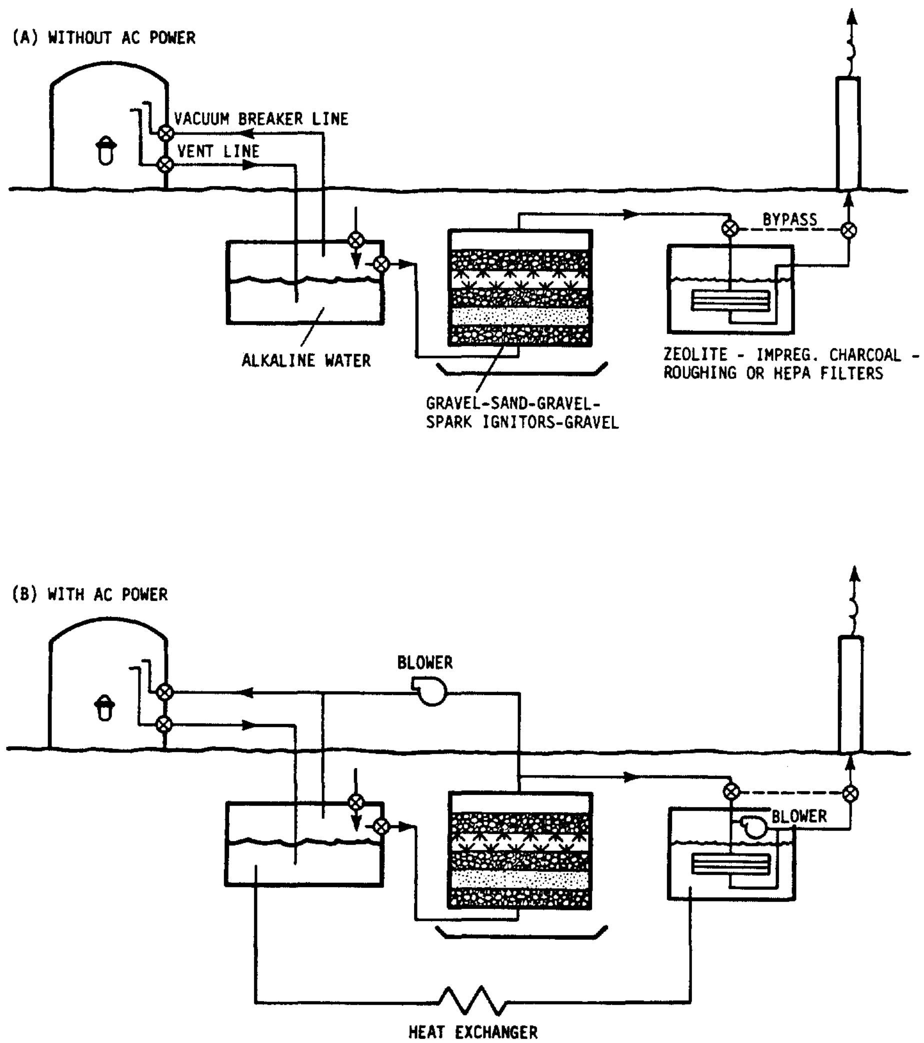

Figure 9 Design Option 4

could be separated by packed fiber. This filter component is designed to be submerged in a 250 m^3 water tank. The water tank would provide passive cooling of the fission product decay heat (during TMLB' accident) from the wafer. The estimated total fission product removal efficiencies for Option 4 are: 99.98% particles, 99.95% I_2, 99.90% CH_3I, 0% Xe and 0% Kr.

Design option 5 is essentially the same as option 4 except xenon holdup is provided for. This requires a thick layer of charcoal trays (1.7 m thick) between the TEDA charcoal and the HEPA filter trays. This option is shown schematically in Figure 10. The estimated total fission product removal efficiencies for Option 5 are: 99.98% particles, 99.98% I_2, 99.98% CH_3I, 98% Xe and 10% Kr.

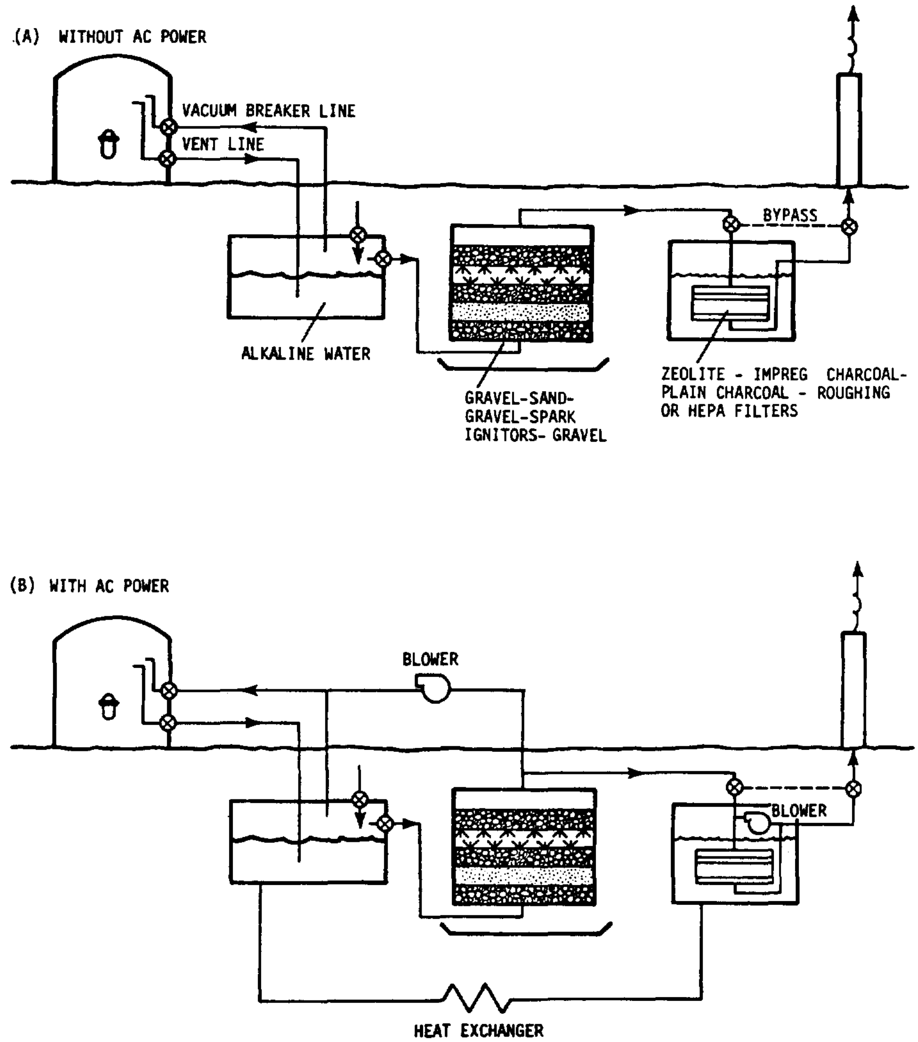

Figure 10 Design Option 5

Design option 6 is a completely contained (no vent to the atmosphere) system. This option is presented in Figure 11. The main features of the system include a toroidal suppression pool and a hydrogen burning area plus a large (30,000 m^3) second containment building. At this volume, the design pressure of the second containment would have to be about 2.8 bar. The hydrogen carried over from the first containment building would have to be burned in the vemt line in order to prevent overpressurization in the second containment due to hydrogen burning there. This option has the potential of holding up all fission products from the damaged reactor. The main disadvantage of this option is the high cost of the second containment building and the difficulty of finding space for this size structure at existing reactor sites.

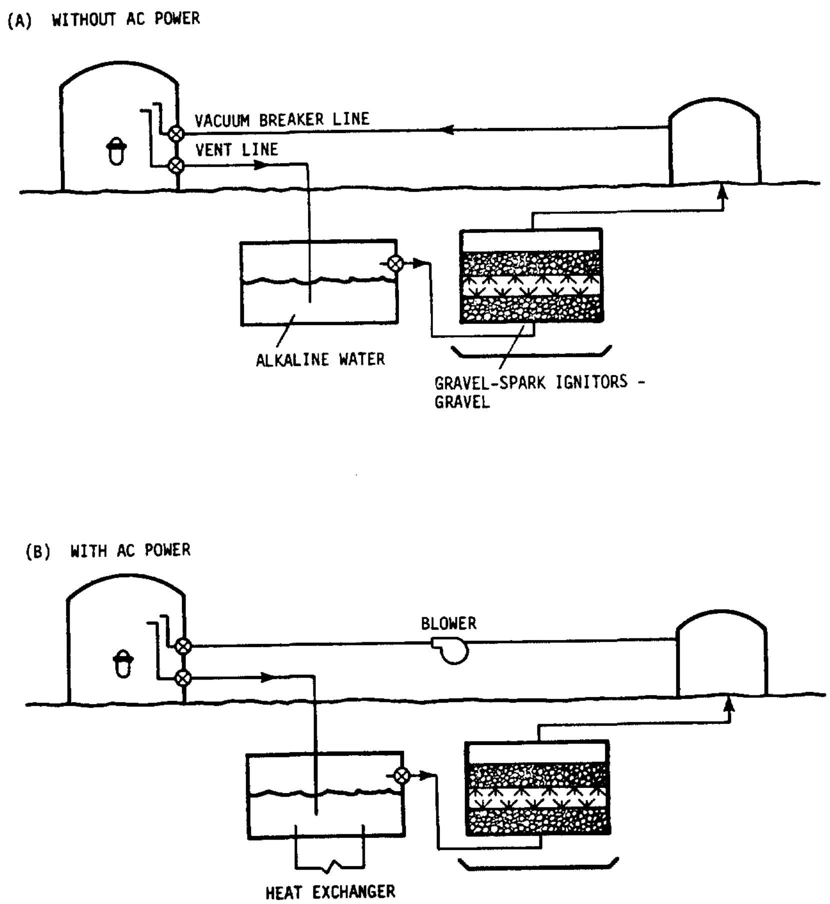

Figure 11 Design Option 6

BWR Design Options

The design options for the baseline BWR are similar to the PWR options except there is no need of a suppression pool since the BWR Mark I has a suppression pool in the primary containment. The option 1 gravel bed would be somewhat larger because it is designed to the heat loads of accident TC.

Consequence Evaluation of the Design Options

An evaluation of the public health consequences using the CORRAL and CRAC computer codes for the TMLB' accident was made. The calculations were made by using the RSS fission product transport and consequence models and the fission product removal efficiencies of the individual design options. Furthermore it was assumed that the containment vessel would be completely failed if there were no FVCS and the filtered-vented containment design options would operate at their predicted efficiencies and prevent containment failure. Weateher and population profiles specific to a densely populated Northeast site were used. The results of those calculations are shown in Figure 12.

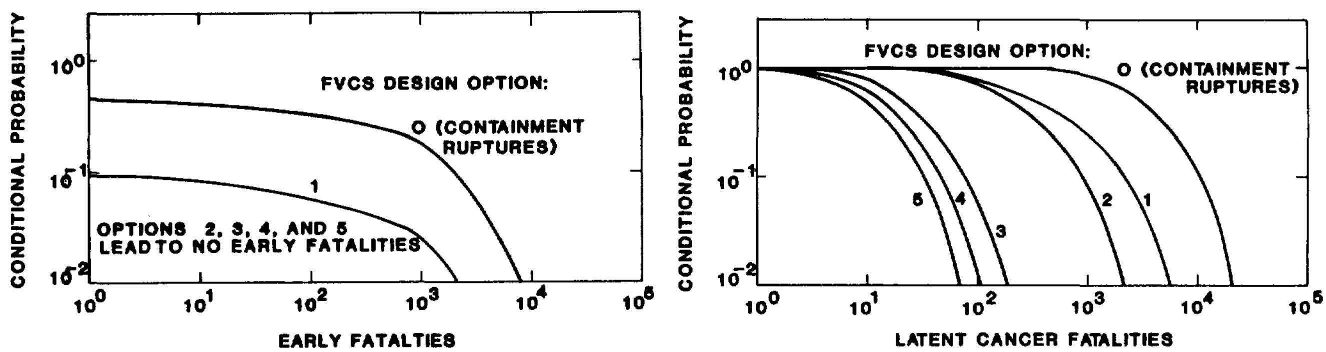

Figure 12 Probability of Early Fatalities and Latent Cancers for TMLB'

Conclusions

Relatively simple filtered-vented containment systems have the potential for significant reductions in reactor consequences. For the particular accident analyzed in the baseline PWR, a single-component system such as a submerged gravel scrubber could provide enough fission product retention to eliminate early fatalities and reduce latent cancer fatalities tenfold, compared to the consequences resulting from an overpressurization rupture of containment. We have estimated that such a system would cost about 16 million U.S. dollars per reactor, but believe that less costly systems with comparable benefits could also be developed. Additional components to contain the noble gases do not appear to be cost effective.

The as-yet unanswered questions are whether or not a complicated venting strategy is necessary in order to circumvent pressure spikes, and whether or not the competing risks would render such a strategy undesirable. We are currently planning experiments to answer the first question and performing a comprehensive probabilistic risk analysis to answer the second. Until these questions are answered, the overall benefits of containment venting remain uncertain.

Acknowledgements

The authors wish to express their appreciation to the people who have made technical contributions to this work. These include Fred T. Harper, David C. Aldrich, Lynn T. Ritchie and Gary J. Boyd at Sandia National Laboratories; Roger O. Wooton and Richard Jung at Battelle Columbus Laboratories; and Roy A Haarman, Dallas T. Pence, and Edward Claiborne at Science Applications, Inc.

References

(1) RASMUSSEN, N. C., et al., Reactor Safety Study, U.S. Atomic Energy Commission, WASH-1400, NUREG-75/014 (1975).

(2) CARLSON, D. D., HICKMAN, J. W., A Value-Impact Assessment of Alternate Containment Concepts, Sandia National Laboratories, SAND77-1344, NUREG/CR-0165 (1978).

(3) CYBULSKIS, P., WOOTON, R. O., DENNING, R. S., Effect of Containment Venting on the Risk from LWR Meltdown Accidents, Battelle Columbus Laboratories, BMI-2002, NUREG/CR-0138 (1978).

(4) GOSSETT, B., et al., Post-Accident Filtration as a Means of Improving Containment Effectiveness, University of California at Los Angeles, UCLA-ENG-7775 (1977).

(5) FINLAYSON, F. C., et al., Evaluation of the Feasibility, Economic Impact, and Effectiveness of Underground Nuclear Power Plants, Aerospace Corporation, ATR-78(7652-14)-1 (1978).

(6) BENJAMION, A. S., Program Plan for the Investigation of Vent-Filtered Containment Conceptual Designs for Light Water Reactors, Sandia National Laboratories, SAND79-1088, NUREG/CR-1029 (1979).

(7) BENJAMIN, A. S. "Filtered Vented Containment System (FVCS) Design Study", Report of the Zion/Indian Point Study, Chapter 1, Sandia National Laboratories, SAND80-0617/1, NUREG/CR-1410 (1980) I-1.

(8) BENJAMIN, A. S., WALLING, H. C., "Development and Analysis of Vent-Filtered Containment Conceptual Deisgns", Thermal Reactor Safety (Proc. ANS/ENS Topical Meeting) CONF-800403/V-1 (1980) 177.

(9) WOOTEN, R. O., AVCI, H. I., A User's Manual for MARCH, A Light Water Reactor Meltdown Accidnet Analysis Code, Battelle Columbus Laboratories, Draft Report (1980).

(10) NORMANN, B., KARLSSON, G., DAMBERG, L., Crushed Rock Filters, Separation with Respect to DOP-Aerosol, Studsvik Energiteknik AB, STUDSVIK/K2-80/332 (1980).

(11) OWEN, R. K., POSTMA, A. K., "Development of a Passive Self-Cleaning Scrubber for Containment Venting Applications", 16th DOE Nuclear Air Cleaning Conf. (1980).

DISCUSSION

HILLIARD: This has been a very interesting discussion. I am sure if we had the time you would be asked a lot of questions about it. I know we have seen a lot of problems connected with this concept.

MILLER: We got involved in some of the studies that were done for Indian Point and Zion, recently, and one of the things that gave us problems was the hydrogen igniter. Have you people done any work on carrying that past the conceptual stage?

WALLING: The best we can do is to try to incorporate the hydrogen ignition, or the hydrogen burn, in the dry gravel and sand filter. You need some type of aftercooling to bring down the temperature.

MILLER: We are concerned that it might pack the gravel and increase the resistance through the bed. You did not give any of the cost factors that you promised at the beginning of the talk.

WALLING: We feel that the simple design option, that is, the submerged gravelbed, following by the dry sand-gravel filter, and then up the stack would cost in the neighborhood of $20 million installed at the baseline PWR site, Zion-Indian Point.

THEORETICAL AND EXPERIMENTAL INVESTIGATIONS INTO THE FILTRATION OF THE ATMOSPHERE WITHIN THE CONTAINMENTS OF PRESSURIZED WATER REACTORS AFTER SERIOUS REACTOR ACCIDENTS

H.-G. Dillmann, H. Pasler
Laboratorium für Aerosolphysik und Filtertechnik GmbH
Kernforschungszentrum Karlsruhe GmbH
Postfach 3640, D-7500 Karlsruhe 1
Federal Republic of Germany

Abstract

For serious accidents in nuclear power stations equipped with pressurized water reactors and with boundary conditions assumed, a conservative evaluation was made of the condition of the atmosphere within the reactor containment, particularly referring to pressure, temperature, air humidity and activity release. Based on these data the loads were calculated of accident filter systems of different designs as a function of parameters such as the course of releases and the volume flow through the filter systems.

A number of experimental results are indicated on the behaviour of iodine sorption materials under extreme conditions including the least favorable temperature, humidity and pressure derived from the calculations above. Reference is made to the targets of future R & D work on aerosol removal.

1. Introduction

Within the frame of reactor safety research it is intended to provide facilities allowing to reduce the releases of activities even in situations involving serious accidents. Therefore, also hypothetical accidents with a highly improbable occurrence are included in the considerations and their possible impacts on the filter systems are evaluated. The studies relate to the possible extent of filter improvement or advancement in such a way that conditions appearing in a hypothetical accident can be controlled.

Fig. 1 shows the venting systems of a German pressurized water reactor. The filters indicated have not been designed for loading by hypothetical accidents. With a view to their use in accidents, filter systems can be developed in two respects:

1. Improved filter systems are used for exhaust air filtering. High removal efficiencies are required for the filter components at high values of temperature, humidity and radiation, since leakages will directly increase the amounts released.

2. Special recirculating air filters are installed, e.g. within the safety containment. The requirements must be even more stringent, because of the physical conditions (temperature, pressure, humidity, radiation) since, as a rule, such a filter must be made operative as early as possible after occurrence of the accident. The removal efficiency might be much lower than for an exhaust air filter because the cleaned air gets mixed again with the containment atmosphere and high decontamination factors can be achieved by repeated filtration.

2. Conditions Prevailing in the Safety Containment

2.1 Development and Reduction of Pressure

The following theoretical work applies to a German 3000 MW_{th} PWR with steel containment (diameter 60 m) and a vented annulus, which can be kept at subpressure with filter systems after an accident to prevent leakages of activities.

According to estimates from [1] and [2] an approximated pressure-time relationship similar to that in Fig. 2 would be obtained in a hypothetical loss-of-coolant accident (LOCA) of a PWR followed by failure of the emergency core cooling system. After a short-term pressure peak during the loss-of-coolant accident a constant pressure level would be attained at 3 bar for approximately one day until the reaction starts between the core melt, the concrete and the sump water.

In this process water vapor and hydrogen would be released from the reaction between the melt and the concrete and metal with water. This again gives rise to a pressure rise which after about some days will attain the theoretical burst pressure of the safety containment. The expected consequence will be the release of a large fraction of fission products into the annular compartment and from there into the atmosphere. One possibility of diminishing this risk consists in reducing the overpressure in the safety containment via a special filter system discharging to the outside. On the basis of the simplified calculation a volume flow from 700 to 3800 m^3/h would be sufficient for this purpose. The intrusion of the sump water onto the melt and concrete of current compositions has been taken into account here. If the intrusion of sump water is avoided and if special dry concretes are used attainment of pressure values jeopardizing the integrity of the safety containment can be delayed up to five to about 30 days. One example (0) was calculated with an air-flow of 15000 m^3/h. In this case it seems to be possible to filter the air by charcoal. More details are given in Fig. 2.

2.2 Assumptions for Estimating the Filter Temperature

An exhaust or recirculating air filter system comprises as a minimum requirement for removal coarse filters, droplet separators, high efficiency particulate air filters (HEPA), iodine filters as well as particulate air filters in series.

In case H_2-resistant adsorption material is not available, the iodine filter must be preceded by H_2-recombiners in addition because of the high H_2-release in core meltdown accidents.

The fission products removed by the filter system generate an additional heat load in terms of decay heat. The filter material so heated is cooled down again by the gas flow. In a first approximation the maximum temperature rises occurring are evaluated on the following assumptions:

The temperatures of the filter material and of the gas are deemed to be equal since the surface to volume ratio is very high.

The noble gases which cannot be removed are not taken into account.

The amounts of the airborne activity - 10 and 20 % of halogenes, 5 and 10 % of the highly volatile given in Tab. 1 and 0.1 % of the low volatile isotopes - are used for the calculations with respect to some plate out and wash out.

The decay rate of the low volatile radionuclides not listed separately was determined in a conservative manner according to Way-Wigner [5]. The β-heat of the removed isotopes was considered to be released by 100 % in the filter, the γ-heat by only 10 %. The filter loading also depends on assumptions made on the time of start-up of operation and on the volume flow through the filter.

In case of homogenuous mixing of the activity the airborne activity is reduced by filtration (leaving out of consideration the radioactive decays calculated to be independent of the respective isotope) in the safety containment, described by the following function:

$$A(x) = A_0 \cdot \exp\left(- \frac{\dot{V}}{V} \cdot [\eta] \cdot t \right)$$

A_0 = theoretical activity concentration at the beginning

$\dot{V}$ = volume flow through the filter

V = volume of the building

η = removal efficiency of the filter

(The factor η is not applicable for exhaust air filter systems.)

Fig. 3 and 4 show the development of off-gas temperature rise for the four volume flows of 700, 1200, 3800 and 15,000 m^3/h determined for pressure limitation. The times of start-up of filter operation at which a pressure in the safety containment of 6 bar is attained are used to calculate the amount of off-gas released.

With the production of off-gas getting smaller the off-gas system must be made operative at later times. However, despite the delayed filter loading with radioisotopes and in spite of the radioactive decay taking place in the meantime, the reduced off-gas volume flows result in higher temperatures.

The maximum temperature rises of about 160^oC above the temperature of about 100^oC of the influent gas. This can be controlled with iodine sorption materials (molecular sieves in the silverform) over a period of 100 h according to the test conducted.

2.3 Radiation Burden

The calculated dose and dose rate values vary over a wide range because only relative arbitrary assumptions can be made on the geometries and activity distributions. However, the magnitudes can be indicated (Fig. 5 and 6).

Also here, apart from 100 % of the β-radiation, 10 % of the γ-radiation were taken into account in the calculations. The dose burdens of the iodine sorption material and of the particulate air filter are indicated.

3. The Efficiency of Recirculating Air Filters

With the burdens to filter systems mentioned above very high decontamination factors cannot be expected according to the present state of the art. Therefore, the efficiency of recirculating air filters installed in the safety containment with respect to a decrease of release in the environment was studied in addition.

In Fig. 7 the efficiency of recirculating air filters is given for three examples of leaks. The rate of leak into the annular compartment is essential for the effect of recirculating air filtering on the level of activity release from the safety containment. Besides the 0.1 cm^2 design basis leak further leaks were studied for their influence on release to take into account the currently used pipe diameters of 80, 100 and 390 mm. Also in this case the vapor-air mixture has to be considered as a medium of transportation. Diffusion through leaks after pressure equalization was neglected.

As expected, it was found that a recirculating air filter is the more effective the smaller the outward leak and the lower the rate of release from the core are. The activity released to the outside might be reduced by up to about two orders of magnitude.

By contrast, if the beginning of release from the core is delayed by about one to two days after occurrence of the accident and if the safety containment is kept sealed, an even much higher reduction in the burden to the environment by recirculating air filters is achieved.

4. Experimental Work

An accident filter basically consists of the following minimum components:

1. coarse separator } (might be combined)
2. droplet separator
3. particulate air filter
4. iodine filter
5. particulate air filter

The technical components such as ventilators, heaters, ducts and fittings will supplement this system.

The filtrating components i.e., the droplet separator, partly the particulate air filter and the iodine sorption unit will be investigated experimentally. Work previously done concerned the iodine sorption unit and the droplet separator as well as the first prototype of the particulate air filter.

4.1 Iodine Sorption Unit

For the iodine sorption unit a material had to be found which has a high removal efficiency for iodine over the whole range of possible conditions and is not characterized by significant desorption also at elevated temperatures and high radiation burden. The activated carbon used in normal exhaust air iodine filters is not eligible because of its easy inflammability and high desorption demonstrated (Fig. 8).

4.1.1 Selection of the Sorption Material. Two materials were tested; firstly, inorganic sorption materials based on catalyzer carriers with a silver nitrate impregnation and, secondly, silver molecular sieves. With both materials the reaction between iodine, iodine compounds and silver gives rise to temperature resistant iodine silver compounds having practically the same desorption behavior. One of the most important parameters influencing removal is the relative humidity (Figs. 9 and 10).

The AC 6120 sorption material contains less silver than the molecular sieves. Already with 7 g Ag/100 g of basic material the removal efficiencies are sufficient at humidities of the air < 80 % RH. Silver zeolites do not attain this value until a silver content of about 30 g/100 g of material has been attained.

4.1.2 Behavior in Humid Air at Ambient Temperatures. In a laboratory scale apparatus tests were performed at different humidities, temperatures and pressures with molecular sieves in the silver form from different suppliers and with impregnated catalyzer carriers (designation AC 6120). Figure 10 shows for the molecular sieve that the penetration is < 10 % at 30°C, 80 % RH and 0.2 s residence time.

The materials must attain minimum removal efficiencies both at high and low temperatures and humidities. This means that design measures have to be taken against droplet storage and reduction in the humidity of the air.

For this purpose, droplet separators with high removal efficiencies must be installed upstream of the filter system and air heaters downstream of it, which over extended periods of operation guarantee a dew point interval of at least 5°C.

4.1.3 Behavior During Pressure and Temperature Rise. The sorption materials behave differently with respect to changes in the parameters of pressure and temperature. Up to a limit temperature of about 250°C the AC 6120 removal efficiency increases with increasing temperature because the reaction rate rises. Above this temperature the impregnation material undergoes thermal decomposition at a relatively high rate (Table II), whilst molecular sieves are more temperature resistant because of the different bonding of the silver in the sorption material.

The removal efficiency decreases with increasing pressure (Table III, measurements made at a constant relative humidity). But this effect is much smaller than the influence exerted by the temperature.

Since the temperature and the pressure are coupled via the vapor pressure curve in a first approximation and since the (positive) influence by the temperature dominates over the influence exerted by pressure, rising pressure will normally not cause a reduction in the removal efficiency of an accident recirculating air filter (Table IV).

For the reasons stated above exhaust air filters will be operated at normal pressure outside the safety containment since throttling will lower the pressure and in addition diminish the relative humidity of the air.

4.1.4 Behavior as Regards Service Life. The service life is an essential parameter with respect to accident filter operation. From the plots showing the development versus time of the airborne activity in the safety containment about 100 hours of safe operation can be expected under conditions of elevated pressure and temperature.

Table IV shows the removal efficiencies as a function of the temperature and time of vapor loading.

Some molecular sieves did not prove to be highly resistant because the binder decomposed. However, as has been shown, some molecular sieves are still capable of meeting with the requirements.

4.1.5 Irradiation Behavior. Dynamic tests with molecular sieves exposed to an air flow were performed at Savannah River Laboratory. The removal efficiencies obtained there were better than the values expected, probably due to the fact that the relative humidity of the air was greatly reduced due to the heat supplied from the dose rate.

A removal efficiency of > 99 % was reached with a 2.5 cm deep bed and 0.1 s residence time while irradiation took place during preconditioning and loading with iodine. Moreover, the desorption was determined over four hours at 1.5×10^7 rad/h [6]. The total dose was 1.6×10^9 rad. The iodine activity desorbed and integrated over 105 hours gave a penetration of 0.7 %.

4.1.6 Behavior with Respect to Hydrogen. Since after a serious accident considerable volume fractions of H_2 might still be present in the containment atmosphere, the influence of hydrogen on the iodine filter must be investigated.

Firstly desorption tests were made on iodine saturated molecular sieves. The temperature range up to 160°C was studied with hydrogen contents of up to 8 % (in nitrogen atmosphere). Under these conditions the desorption rate (after five hours) was $< 10^{-5}$ % of the iodine loading. The value of 10^{-5} corresponds to our detection limit. In the near future removal tests will be performed with HI.

4.2 Particulate Air Filter

At the time being, reliable statements cannot be made on the behavior of particulate air filters exposed to both elevated pressure, high temperature and high humidity of the air. From experience gathered by users and laboratory tests, respectively, it is merely known that particulate air filters when exposed to air saturated with humidity and with water droplets exhibit a sharply rising differential pressure and might rupture when storing water, above all after extended service lives. Basic investigations covering all these conditions have not yet been made because presently no methods exist of filter testing when the parameters indicated exert an influence at the same time.

Also under this test program several prototype filters of mats of 4 µm stainless steel fibers were built and investigated.

The first results have yielded removal efficiencies between 99.94 and 99.95% with a flow rate of 20 cm/s vertical to the fiber axis and a test aerosol with a frequency of abundance at a particle diameter of 0.1 µm (uranin). For the 30 layers of metal fibers used the pressure drop was about 120 mm of water gauge. Filters of this type are not burnable, unaffected by temperature, high humidity of the air, droplets, pressure surges and radiation.

4.3 Demister

Above all two boundary conditions are decisive for the use of a droplet separator.

1. Great quantities of water must be expected since in an accident up to about 300 tons of water get released and when escaping a large volume of it is in the vapor phase and recondenses subsequently.

2. Over a rather long period during the condensation phase very small droplets must be expected which might lead to an inadmissible storage of water in the particulate air filters and in the iodine filter.

Moreover, a droplet separator must have the lowest possible resistance to air and must be radiation resistant.

These conditions can be fullfilled by using demisters made of stainless steel fiber separators. Such fibers are presently offered with diameters of 22,12, 8 and 4 µm. After optimization a configuration of droplet separators of 22 and 8 µm fibers by four layers each has proved to be suitable for use in coarse and fine droplet separators. The results have been indicated in Table V.

4.4 Technical components

Technical components are understood to include heaters and driving systems (ventilators and motor). The versions offered by industrial firms are suited for operation in the expected range of parameters.

5. Conclusions

Already at the planning stage filter systems for hypothetical accidents must be taken into account for a nuclear power station because they derivate from usual filters in their design (separate discharge network, stand-by function, maintenance during and after serious accidents). Their flow capacity must be optimized with a view to the boundary conditions to be assumed. Inadequate volume flows might result in loading of the filter materials by decay heat and radiation doses up to values which can no longer be controlled. Oversized systems require excessively high costs for the sorption material, blower, blower performance and space required.

The filter system should be equipped with a droplet separator and a preheater installed in the direction of flow so that the filter media during permanent operation are not exposed to more than 80 % of relative humidity of the air. In case of recirculating air filtering the particulate air filters should furnish a removal efficiency of at least 90 % and be unaffected by humidity, whilst for exhaust air filters removal efficiencies of $>$ 99,9 % should be reached.

In case of recirculating air filters the iodine sorption filter should have a residence time of 0.2 s for 5 cm bed depth and be filled with silver molecular sieves.

Exhaust air filters call for much higher residence times than recirculating air filters ($>$ 1 s) in order to attain higher removal efficiencies.

The configuration can be of flat beds, but other geometries are conceiveable as well. To support thermoconvection a stack type exhaust air outlet of at least 10 m height should follow a filter, which supports the fans and provides a minimum air flow for filter cooling and for maintaining the filter performance in cas of failure of the fan. A complicated discharge network is certainly not appropriate because of the pressure drop.

The required volume flow will be distributed to more parallel systems (redundancy). This also allows to select a simple layout for the safety containment.

To make exhaust air filters universally applicable after serious accidents they should be connected so that they can ventilate the different spatial areas such as safety containment and annular rooms (in case of major leakages).

The high price of silver should not be an argument against silver molecular sieves because the silver of the slowly aging sorption material in the stand-by filters, can be recovered with low costs. It is only in case of an accident that the silver cannot be recovered.

References

[1] The erosion behavior of different types of concrete interacting with a core melt. M. Reimann IRB/KFK
Proc. Thermal Reactor Safety April 6-9, 1980 Knoxville, Tenn. p. 197-204

[2] personal communication,
Project Nuclear Safety (PNS), KfK.

[3] KfK 2262 PNS-Halbjahresbericht 1975/2, S. 109 ff.

[4] Störfall-Umluftfilter in Kernkraftwerken. Stand der Entwicklung.
LAF, PNS, unveröffentlicht.

[5] D. Smidt, Reaktortechnik Bd. 1
G. Braun Verlag, Karlsruhe, 1971.

[6] A. G. Evans, Savannah River Laboratory
15th DOE Nuclear Air Cleaning Conference
Boston, 7.-10. Aug. 1978, S. 416 pp.

[7] J.G. Wilhelm, Behaviour of Iodine Sorption Materials, Seminar on Iodine Filter Testing, CEC Doc. V/559/74 (Nov. 74).

Tab.I: Isotopes taken into account in the calculations.

The output is related to a decay time of 100 sec, a thermal power of 3000 MW and a full power operation of 3 years

isotope	half-life-time	output (W)	output (W)
(halogenes)		β	γ
I 130	12.36 h	$5.6 \cdot 10^{-2}$	$1.6 \cdot 10^{-1}$
I 131	8.04 d	$8.8 \cdot 10^{4}$	$1.7 \cdot 10^{5}$
I 132	2.38 h	$3.4 \cdot 10^{5}$	$1.6 \cdot 10^{6}$
I 133	20.8 h	$4.1 \cdot 10^{5}$	$6 \cdot 10^{5}$
I 134	52.0 min	$5.5 \cdot 10^{5}$	$2.1 \cdot 10^{6}$
I 135	6.59 h	$3.6 \cdot 10^{5}$	$1.3 \cdot 10^{6}$
highly volatile isotopes			
Se 81^{m}	18 min	$5.71 \cdot 10^{2}$	$7.5 \cdot 10^{-1}$
Se 83	22.4 min	$1.2 \cdot 10^{4}$	$6.9 \cdot 10^{4}$
Rb 88	17.8 min	$9.2 \cdot 10^{5}$	$4.2 \cdot 10^{5}$
Rb 89	15.2 min	$5.3 \cdot 10^{5}$	$1.4 \cdot 10^{6}$
Sr 89	50.5 d	$3.2 \cdot 10^{5}$	$4.6 \cdot 10^{3}$
Sr 90	28.5 yr	$9.6 \cdot 10^{3}$	-
Sr 91	9.5 h	$4.4 \cdot 10^{5}$	$5 \cdot 10^{5}$
Sr 92	2.71 h	$1.7 \cdot 10^{5}$	$9.5 \cdot 10^{5}$
Ru 103	39.35 d	$3.6 \cdot 10^{4}$	$2.7 \cdot 10^{5}$
Ru 105	4.44 h	$1.5 \cdot 10^{5}$	$2.4 \cdot 10^{5}$
Ru 106	368 d	$2.5 \cdot 10^{3}$	-
Te 127	9.35 h	$9 \cdot 10^{3}$	$3.8 \cdot 10^{4}$
Te 129	69.6 min	$7.1 \cdot 10^{4}$	$2.8 \cdot 10^{4}$
Te 131	25.0 min	$3.1 \cdot 10^{5}$	$1.5 \cdot 10^{5}$
Te 133	12.5 min	$2.7 \cdot 10^{5}$	$9 \cdot 10^{5}$
Te 133^{m}	55.4 min	$5.2 \cdot 10^{5}$	$1.1 \cdot 10^{4}$
Te 134	41.8 min	$1.3 \cdot 10^{5}$	$5.4 \cdot 10^{5}$
Cs 134	2.06 yr	$2.5 \cdot 10^{4}$	$2.5 \cdot 10^{5}$
Cs 137	30.1 yr	$1.2 \cdot 10^{4}$	-

Tab. II: Comparison of the iodine sorption materials AC 6120 and Ag - molecular sieves

at different temperatures, pressures and dew point temperatures

test agent :ca. 1.5 mg/g $CH_3{}^{127}I$ + 1 mCi $CH_3{}^{131}I$

iodine sorption-material :AC 6120 with ca. 8 g Ag/100 g base material; molecular sieve with ca. 30 g Ag/100 g base material

bed depth :ca. 10 cm

test gas :superheated steam

residence time :ca. 0.4 sec

flow :ca. 440 l/h

pressure (bar)	test-bed temperature (°C)	dew point temperature (°C)	removal efficiency (%) AC 6120	Molecular sieves	test duration at high temperature (h)
1	110	102-105	99.993		1-2
1	130	103-105	99.998	99.996	1-2
1	150	105	99.999	99.993	1-2
5	160	150	99.984	99.921	1-2
5	200	150	99.979	99.977	7
5	300	150	99.75	98.6	7

Tab. III : Removal efficiency in dependence of temperature and pressure

material :AC 6120, test duration 1 - 2 h

flow :800 m^3/h

residence time :0.2 sec

rel. humidity :70 %

test agent :ca. 5 mg CH_3I + 1 mCi $CH_3{}^{131}I$

temperature (°C)	pressure (bar)	removal efficiency (%)
30	1	99.5 +)
30	3	99.4
30	5	97.4 +)
120	2	99.998+)
120	5	99.95 +)

+) average of different tests

Tab. IV: Removal efficiency of an Ag molecular sieve for $CH_3{}^{131}I$ under extreme conditions

face velocity: 25 cm/sec

loading time : 5 min

purging time : 2 h

temperature (°C)	dew point temperature (°C)	pressure (bar)	exposure time (h)	removal efficiency (%) bed depth (cm)	
				2.5	5.0
150	105	1.2	5 96	99.2 99.9	99.99 99.99
160	151	5	5 96	96.0 95.4	99.77 99.71
300	151	5	5 96	97.8 83.9	99.89 97.4

Tab. V: Removal efficiency of a droplet separator containing stainless steel fiber packs

diameter of droplets: 2-5 μm

loading rate : ∿ 3 kg/h

fiber diameter

pack 1 : 22 μm

pack 2 : 8 μm

air flow rate (m^3/h)	face velocity (m/sec)	total pressure drop (Pa)	removal efficiency (%)		
			pack 1	pack 2	packs 1 + 2
200	0.23	250	99.6	98.9	99.996
300	0.34	320	99.4	97.3	99.98
400	0.46	480	99.5	89.3	99.94

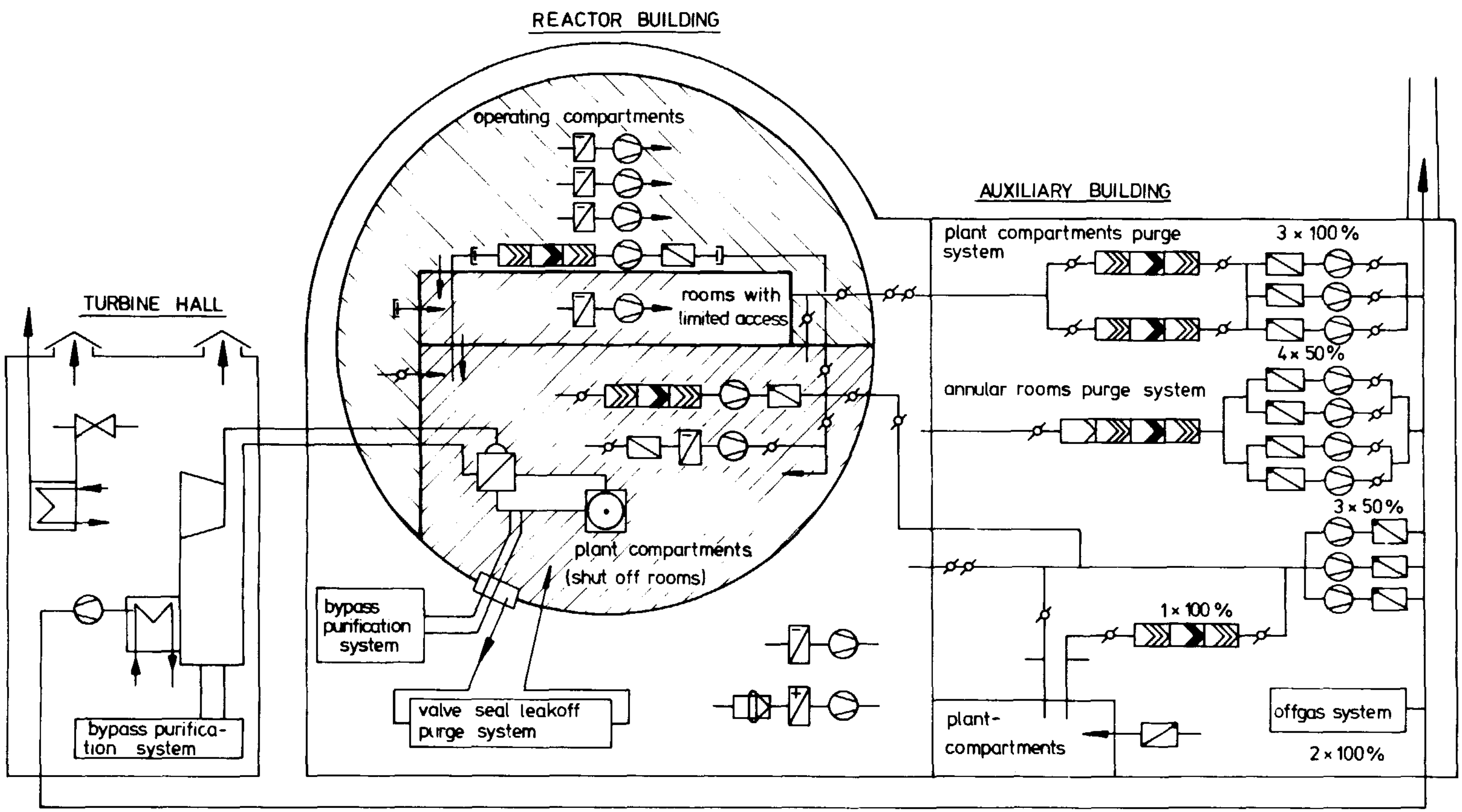

Ventilation system of a German PWR

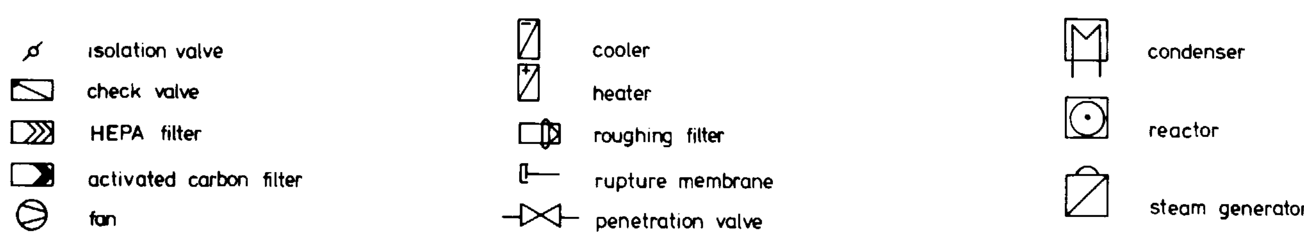

Fig. 1

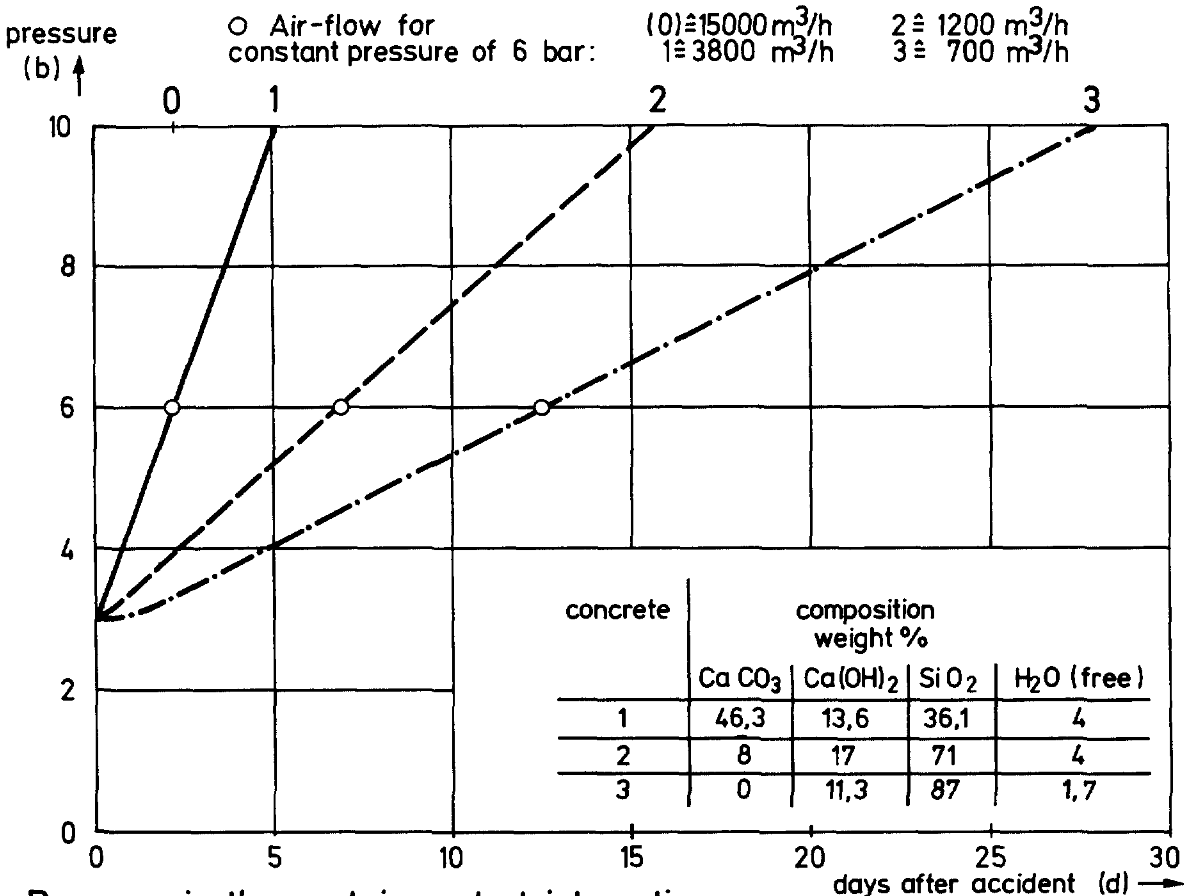

concrete	composition weight %			
	Ca CO_3	Ca$(OH)_2$	Si O_2	H_2O (free)
1	46,3	13,6	36,1	4
2	8	17	71	4
3	0	11,3	87	1,7

Pressure in the containment at interaction of concrete and melt as a function of time
(calculatet by M.Reimann IRB/KfK with „Wechsel")

Fig. 2

Example

0 gives the possibility to filter the containment by higher gas flow with charcoal by the same airborne activity as in example 1-3 also by earlier start time of filter operation.

1 gives the pressure rise by reaction of a average american concrete with melt and without sump water and a middle german concrete with melt and sump water.

2 gives the pressure rise by reaction of a german concrete with melt and no contact with sumpwater.

3 gives the pressure rise by reaction of a theoretical concrete with melt and without sumpwater.

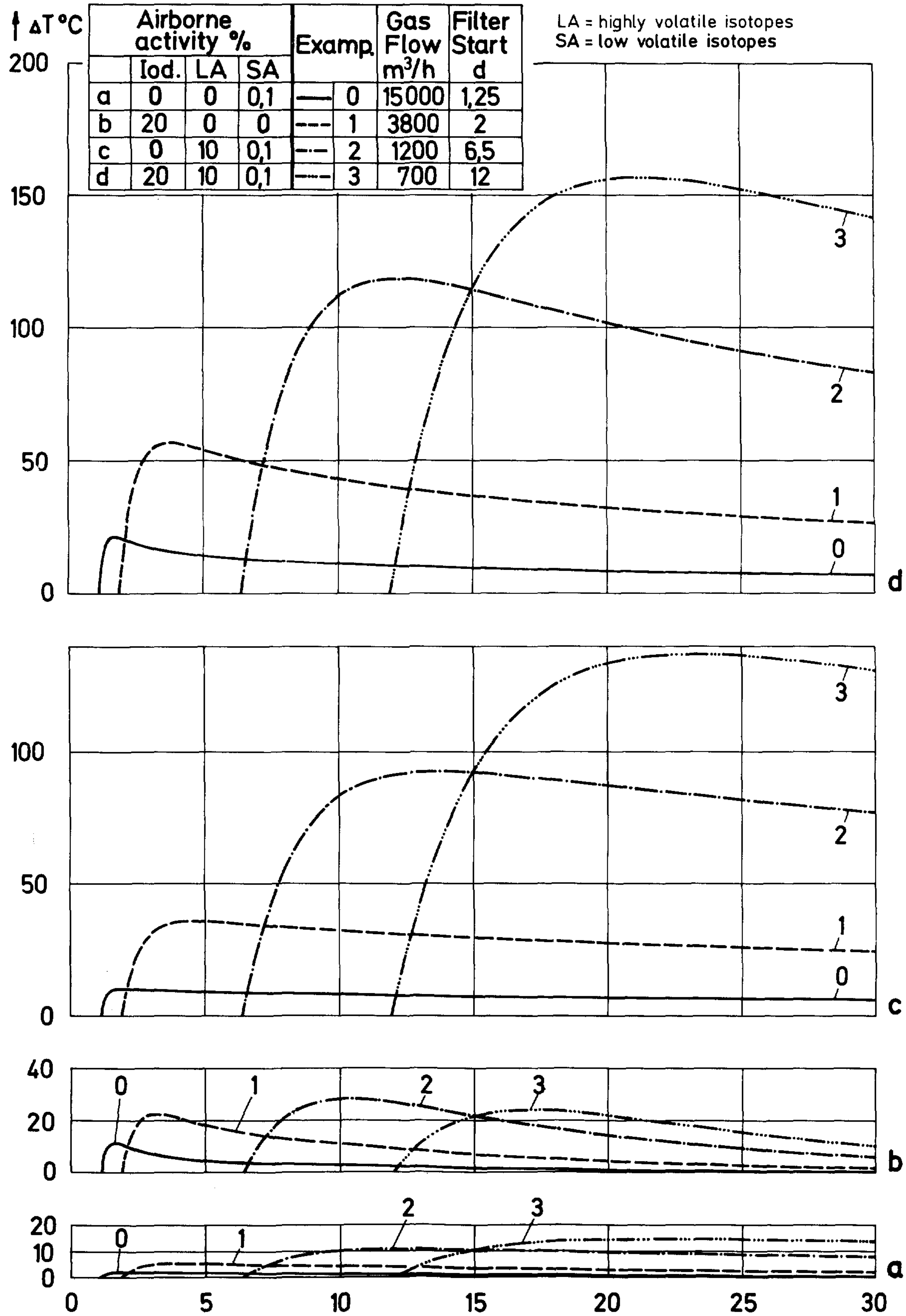

	Airborne activity %			Examp.		Gas Flow m³/h	Filter Start d
	Iod.	LA	SA				
a	0	0	0,1	——	0	15000	1,25
b	20	0	0	- - -	1	3800	2
c	0	10	0,1	—·—	2	1200	6,5
d	20	10	0,1	—··—	3	700	12

Temperature rise of exhaust air filter system after an accident as a function of time

Fig. 3

d

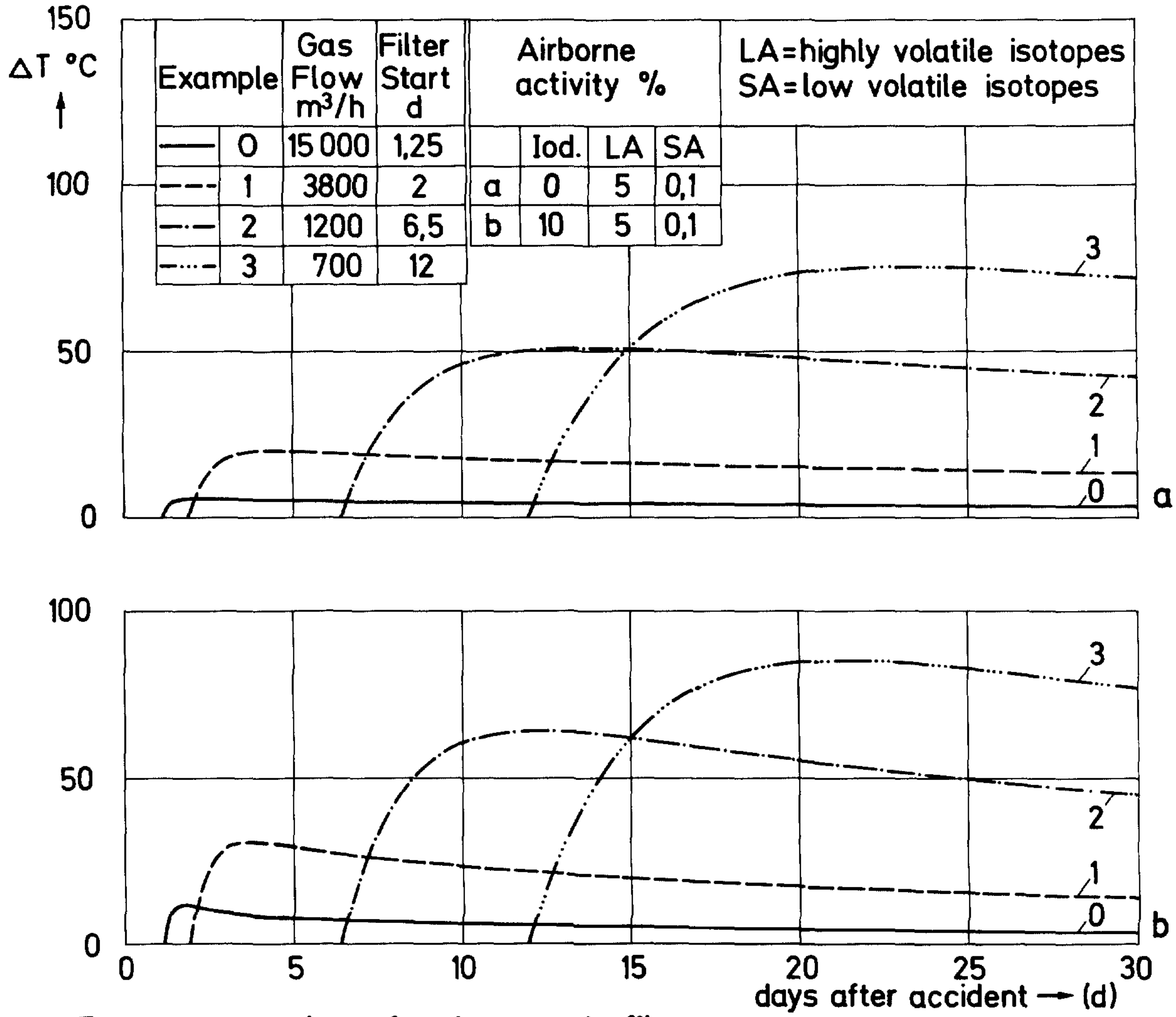

Temperature rise of exhaust air filter system after an accident as a function of time

Fig. 4

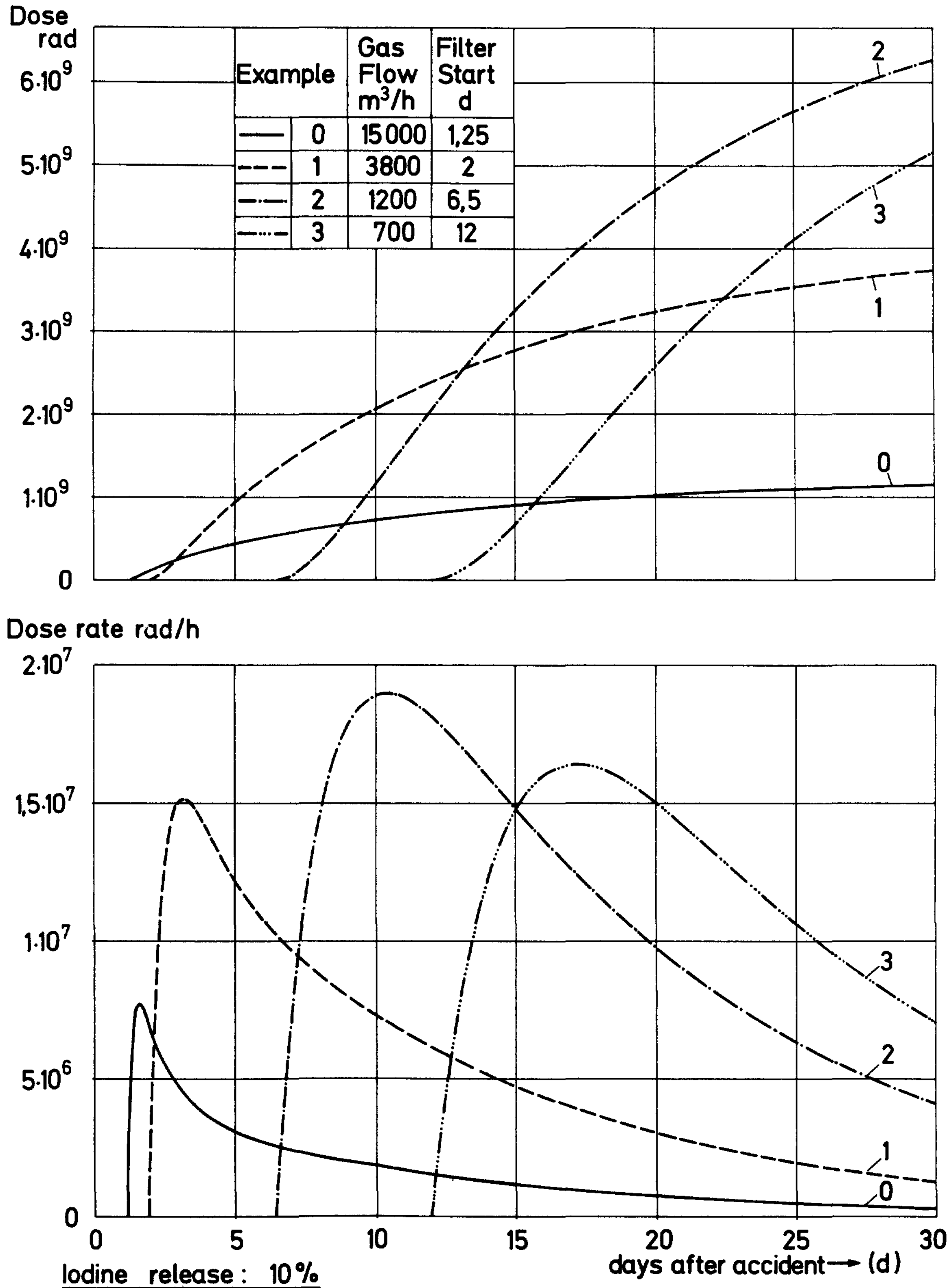

Dose and Dose rate of the iodine filter after an accident as a function of time

Fig. 5

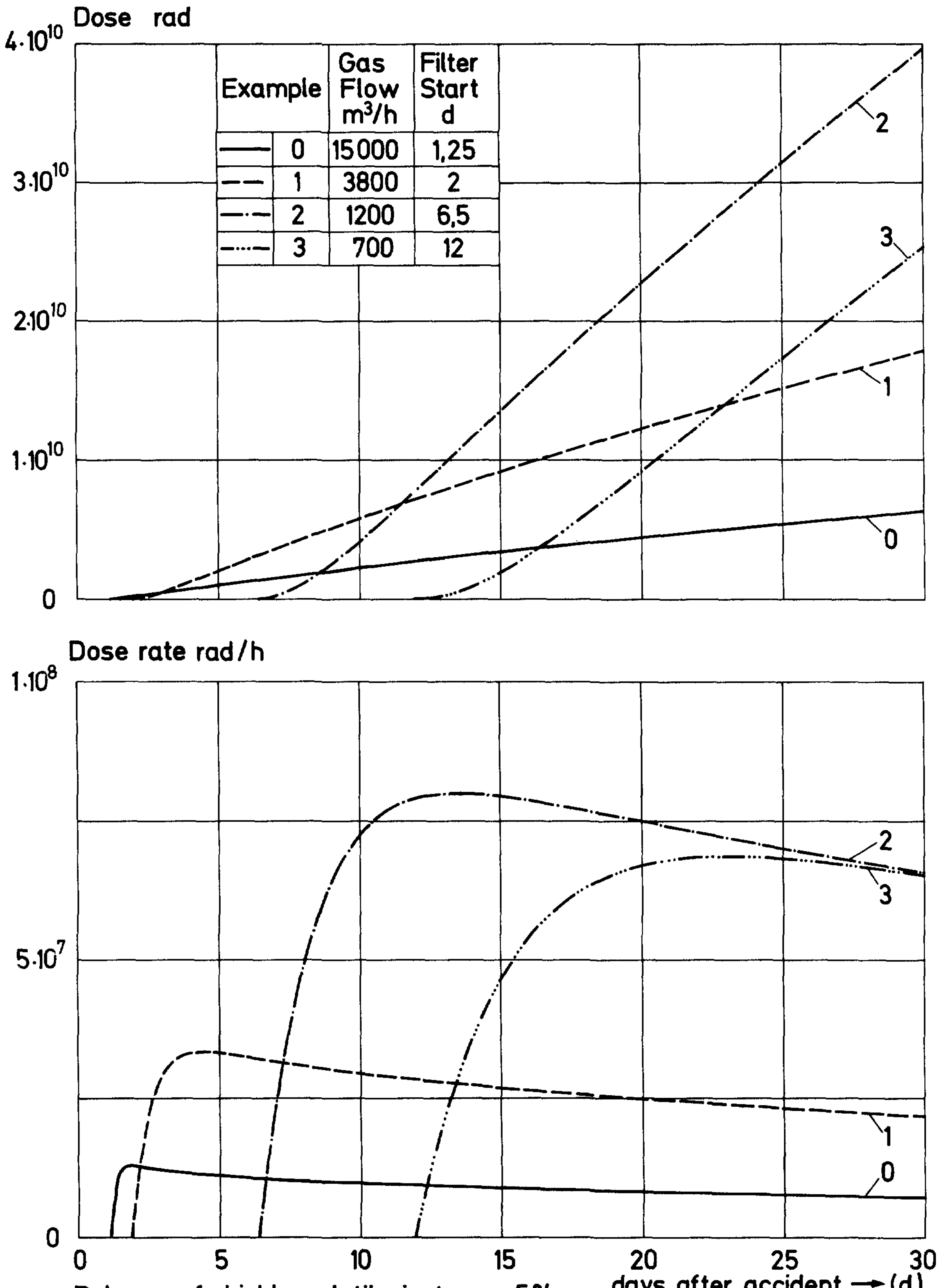

Release of: highly volatile isotopes 5%
low volatile isotopes 0,1%

Dose and Dose rate of the HEPA filter after an accident as a function of time

Fig. 6

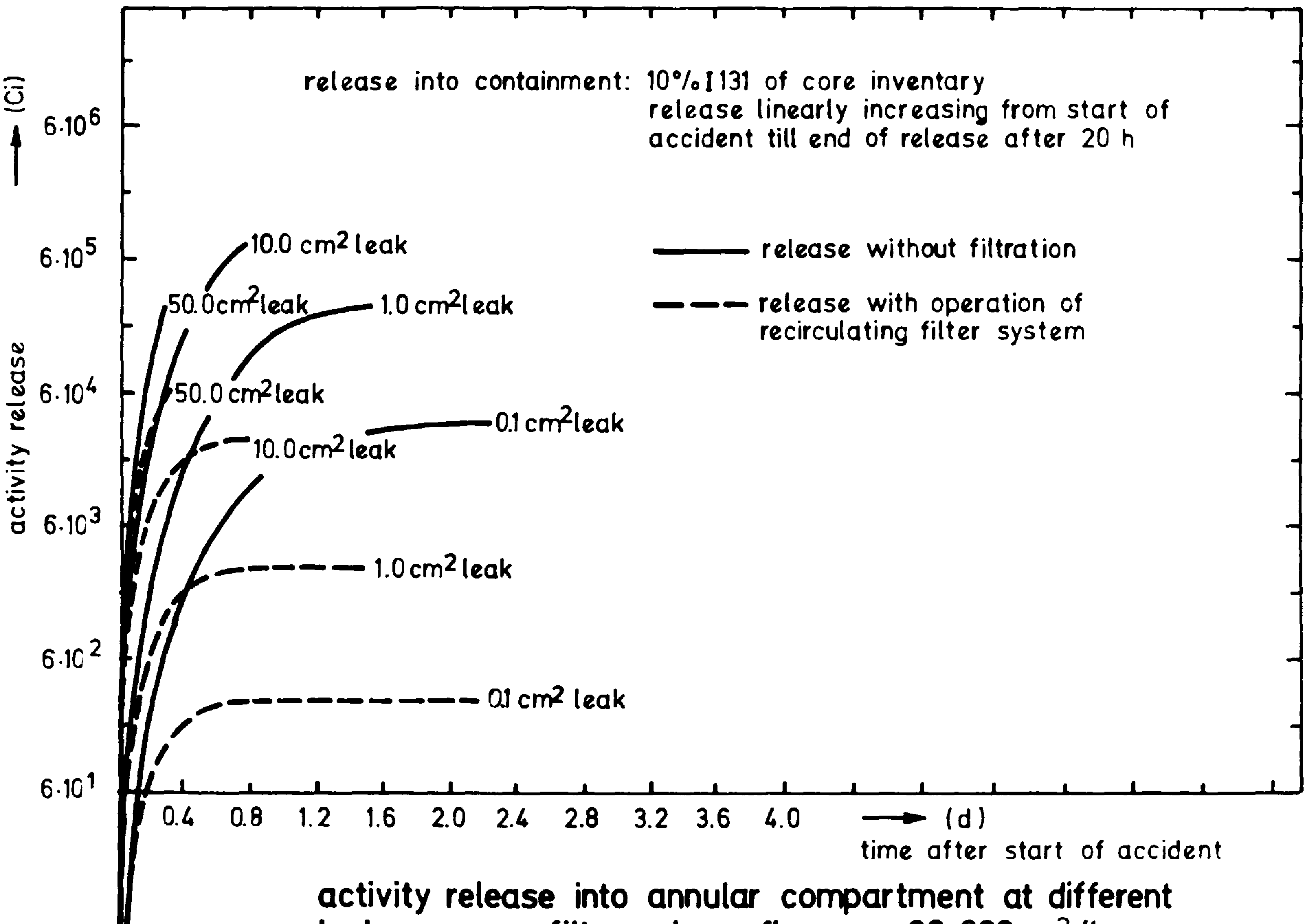

activity release into annular compartment at different leak aereas - filter volume flow = 20 000 m^3/h

Fig. 7

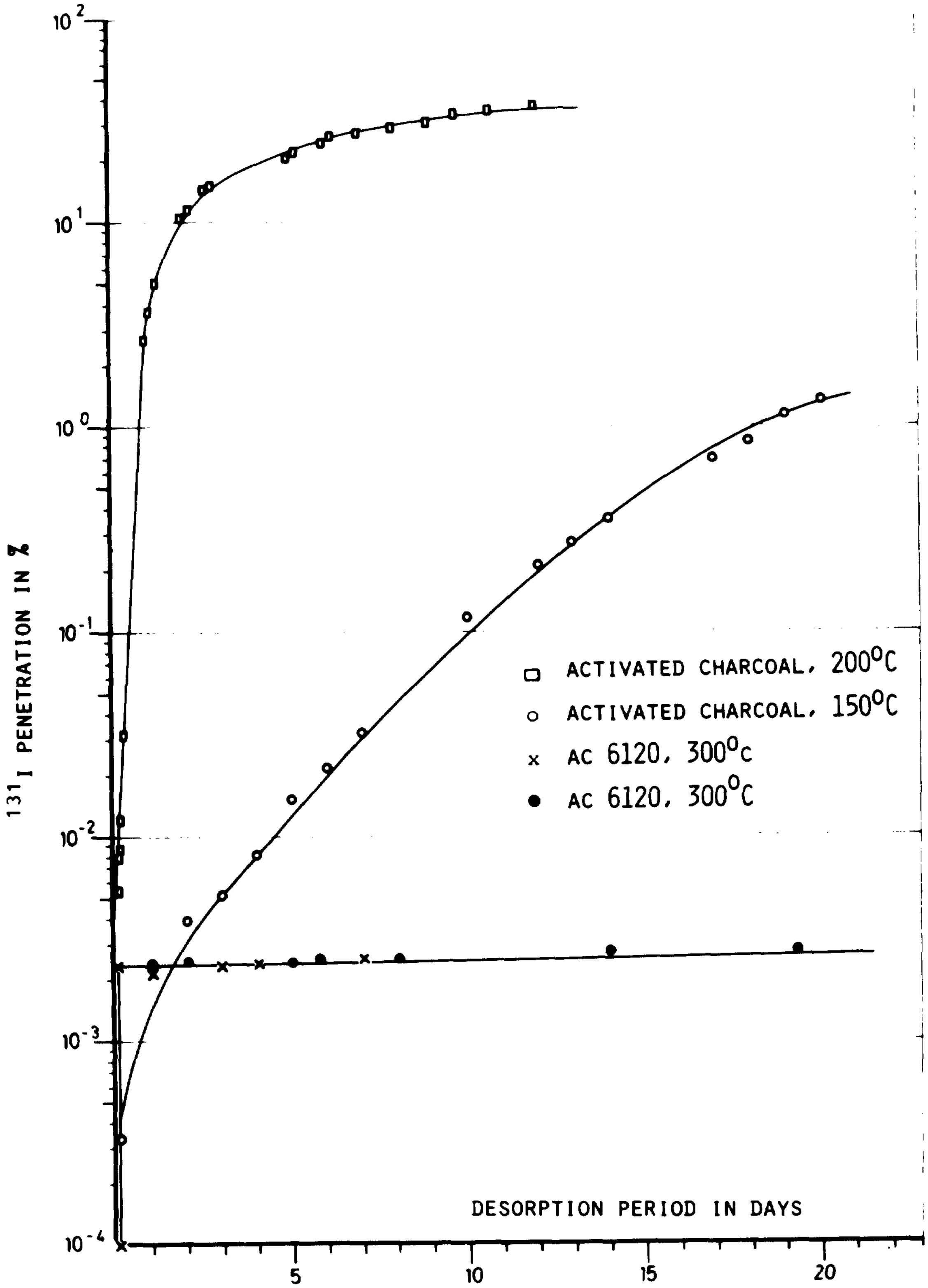

^{131}I DESORPTION OF VARIOUS ADSORBERS AT ELEVATED TEMPERATURES 7)

FIG. 8

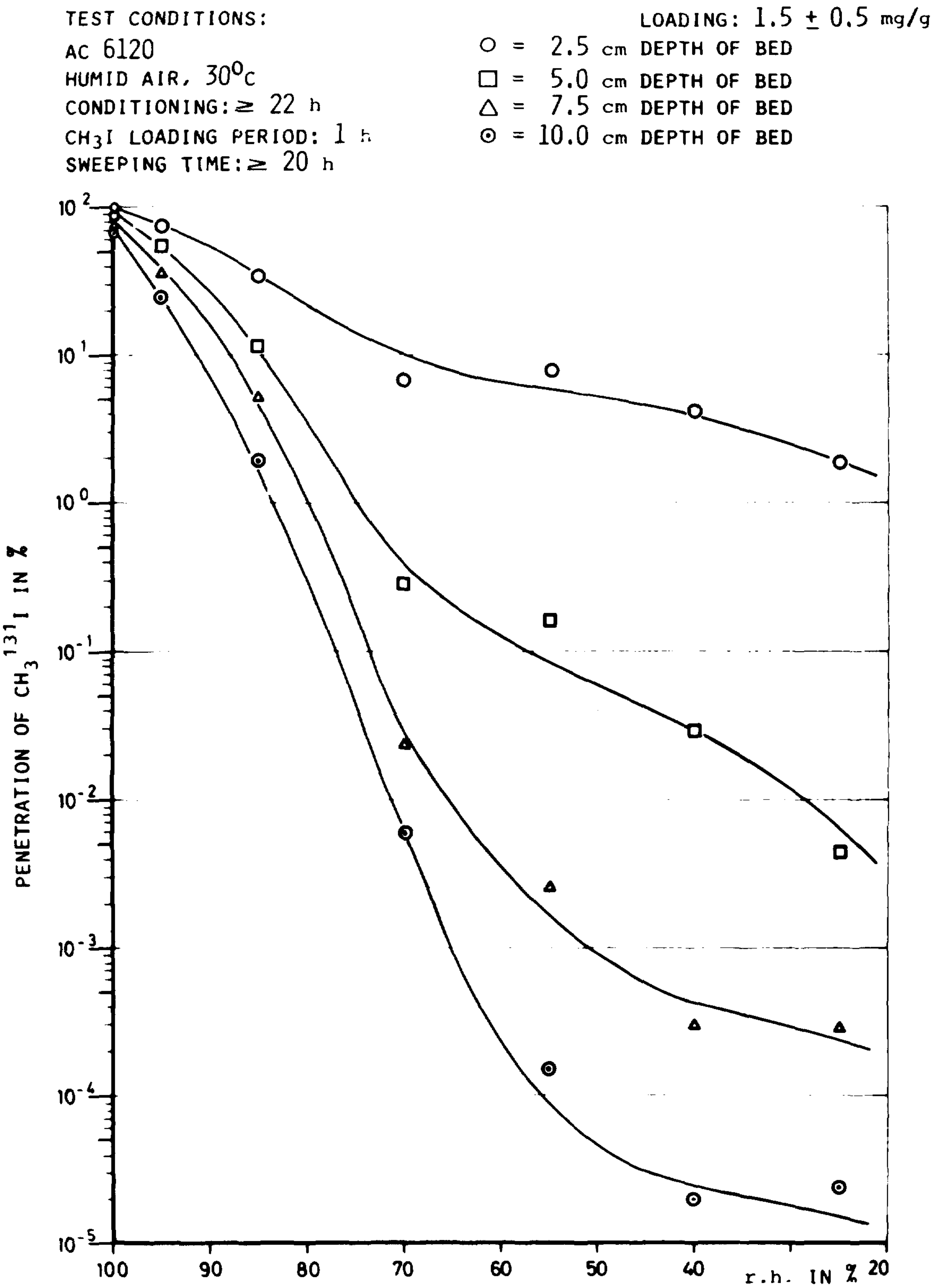

PENETRATION OF AC 6120 BY $CH_3{}^{131}I$ AS A FUNCTION OF THE RELATIVE HUMIDITY OF THE AIR 7)

FIG. 9

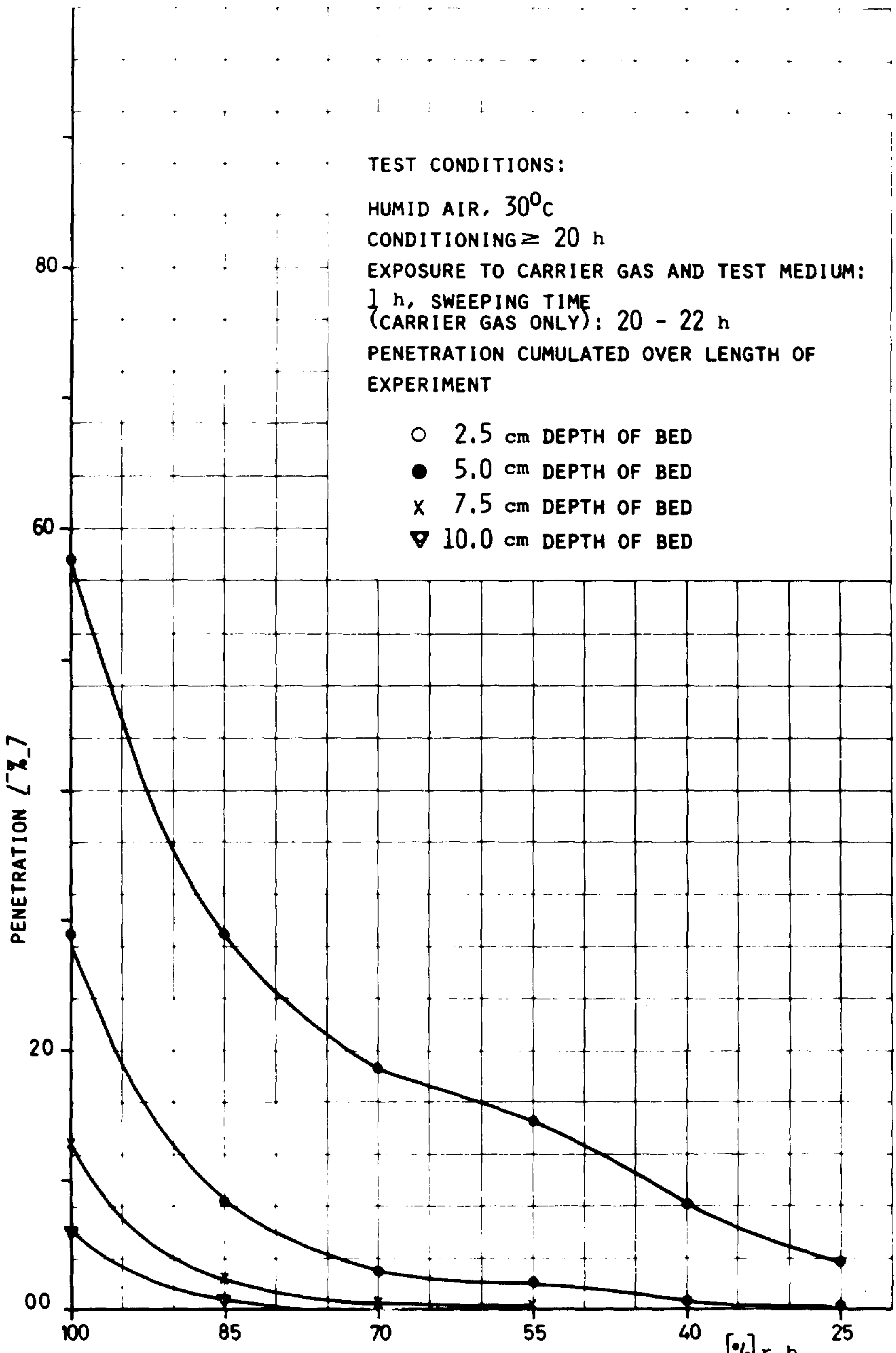

PENETRATION OF LINDE 13 X Ag BY $CH_3{}^{131}I$ AS A FUNCTION OF THE RELATIVE HUMIDITY OF THE AIR 7)

FIG. 10

DISCUSSION

JEFFORD: How long following an accident do you expect your filters to keep operating?

DILLMAN: In the third Figure, I gave the starting points of the filter systems. The total time was thirty days in my calculation. For a starting point of 1.25 days, there will be a high volume flow of 15,000 m^3/hr. This is shown in Example 0. Example 1, is for 3,800 m^3/hr. and starts after two days. Example 2 starts after 6.5 days with 1,200 m^3/hr. The last example is a theoretical concrete, not a real concrete, and this starts after 12 days with a flow rate of 700 m^3/hr.

JEFFORD: In the testing of your silver zeolite, you specified loading for a very short period of time and testing for an hour or so. How well do you think that sort of testing will reflect the 30-day lifetime, or operational period, of your filters?

DILLMAN: In the table giving the lifetime of the molecular sieves, we have given the data for 100 hours of testing under high temperature and pressure. These will be very strong conditions, because under filter operations the pressure will be near 1 bar. The decrease of efficiency is not so high that we think that this filter material, molecular sieve in the silver form, will operate for a longer time.

JEFFORD: So you believe 100 hours is a reasonable indication that the molecular sieves will last for 30 days with no problem. Is that right?

DILLMAN: I think so.

LARGE-SCALE TESTS OF AQUEOUS SCRUBBER SYSTEMS FOR LMFBR VENTED CONTAINMENT

J. D. McCormack, R. K. Hilliard and A. K. Postma
Hanford Engineering Development Laboratory
Operated by Westinghouse Hanford Company
Richland, Washington 99352

Abstract

Six large-scale air cleaning tests performed in the Containment Systems Test Facility (CSTF) are described. The test conditions simulated those postulated for hypothetical accidents in an LMFBR involving containment venting to control hydrogen concentration and containment overpressure.

The CSTF is a 850-m^3 steel vessel within which various types of sodium aerosols are generated and characterized to provide an aerosol source for air cleaning tests. In the present test series, the aerosol was generated over a 30-hr period of time by continuously spraying sodium into air. Steam and/or carbon dioxide was added to create the desired Na_2O_2, Na_2CO_3 or NaOH aerosol. Suspended concentrations up to 50 g/m^3 and particle sizes from 1.1 to 6.5 μm aero dynamic mass median diameter were tested.

Two air cleaning systems were tested: (a) spray quench chamber, eductor venturi scrubber and high efficiency fibrous scrubber in series, and (b) the same except with the spray quench chamber eliminated. The gas flow rates ranged up to 0.8 m^3/s (1700 acfm) at temperatures to 313°C (600°F). Quantities of aerosol removed from the gas stream ranged up to 700 kg per test.

The systems performed very satisfactorily, with overall aerosol mass removal efficiencies exceeding 99.9% in each test. Information is presented on deposition of aerosol in inlet ducts and other operational behavior.

I. Introduction

An air cleaning development program is in progress at the Hanford Engineering Development Laboratory (HEDL) which has the objective of developing and demonstrating, at a large scale, air cleaning systems for application in LMFBR plants during hypothetical accident conditions. Because LMFBR accidents involving very high sodium aerosol concentrations can be postulated, a requirement of the air cleaning system is that it have high mass loading properties (to 10^5 kg) as well as high removal efficiency (>99%) for aerosol particles.

An evaluation of current air cleaning technology as applied to postulated LMFBR accident conditions showed that aqueous scrubbers had the best potential for meeting the requirements, but that no single scrubber could attain the dual requirement of high mass loading and high efficiency.(1) Therefore, a system comprised of several types of scrubbers in series was selected for demonstration. Four tests, (AC1-AC4) were performed with a 3-stage scrubber system and two tests (AC5-AC6) with a 2-stage system.

The test aerosol in all six tests was generated by spraying sodium continuously into an air filled model containment vessel to create various chemical forms of sodium aerosols. It is generally agreed that aged aerosols of differing source materials will coagglomerate so that all individual particles have the same chemical composition. Thus, in an accident where radioactive substances were released along with the sodium, condensible radioactive materials would nucleate and form solid or liquid aerosol particles which would rapidly co-agglomerate with the sodium aerosol particles. Because the sodium mass concentration greatly exceeds that of the radioactive material, the transport and deposition behavior of the multi-component aerosol is nearly identical to that of sodium-only aerosol. An exception to this concept of uniform aerosol composition could develop if a volatile, condensible fission product compound, e.g., NaI, existed as a vapor in the containment atmosphere but nucleated to very small particles during passage through a scrubber system. An evaluation of the removal of NaI vapor in an aqueous scrubber system showed that a 3-component system such as was tested in the present work would remove $>$ 97% of the NaI.(2) To confirm this calculation, NaI vapor was added to the scrubber inlet in tests AC-3 and AC-4.

In one test (AC-5), the system was operated at degraded flow conditions to demonstrate the effect on scrubber efficiency and pressure drop. The results of all six tests are discussed in this paper.

II. Experimental Arrangement

Test Facility

The large-scale demonstration tests were performed in the Containment Systems Test Facility (CSTF). The chief feature of the CSTF is an 850-m steel containment vessel, 20.3 m high. The CSTF has been described previously.(3, 4, 5) Up to 1250 kg of sodium can be discharged into the containment vessel to create a pool or spray fire aerosol source. For the tests discussed in this paper, the aerosol was generated by continuously spraying sodium for approximately 30 hr with an air atmosphere in the containment vessel. In some tests, steam and/or carbon dioxide was injected to simulate the release of gas and water vapor from concrete heated by the accident thermal conditions.

Test Articles

The three-component scrubber system used in tests AC-1 through AC-4 consisted of a quench tank (QT), an eductor venturi scrubber (VS), and a high efficiency fibrous scrubber (FS) in series. A flow diagram is shown in Figure 1 and a photograph of the system as installed in the CSTF is shown in Figure 2. In tests AC-5 and AC-6, the quench tank was removed and only the venturi and fibrous scrubbers were used, as shown in the flow diagram, Figure 3. One other difference in the two test series was that the inlet duct leading from the containment vessel to the scrubber system exited from low in the containment for the first four tests and from high in the containment for the last two. This change was made to be more comparable to an actual plant design, but had no effect on the performance of the scrubbers. Details of the three scrubbers are shown in Figure 4.

Quench Tank. The purpose of the QT was to cool hot gases received from the containment vessel. Either of two banks of 1/2-G26* aqueous spray nozzles was operated at various flow rates. The spray drop size was 2600-μm AMMD. A 2.15-m^3 liquid holdup tank and pump were provided. The vessel was fabricated of carbon steel with unpainted interior surfaces. Although intended to act primarily as a gas cooler, the QT also served to remove the larger aerosol particles and to humidify the gas.

Venturi Scrubber. The purpose of the VS was to reduce the aerosol concentration sufficiently so that the fibrous scrubber would not plug. The VS was a jet ejector type, providing 250 Pa pressure gain when operated at 3.2 l/s liquid rate and 0.47 m^3/s gas flow rate. All gas flow rates in this paper are measured at standard conditions of 0°C, 1 atmosphere. The design particle removal efficiency was 90% for 5-μm AMMD, 3.0 σ_g aerosol. A liquid storage tank and recirculating pump was provided. The VS, 2.15-m^3 tank, pump and lines were carbon steel.

Fibrous Scrubber. The FS consisted of a 5.8-m^2 polypropylene fiber element mounted within a steel housing. The fiber element was a 610-mm OD by 3050-mm length hollow cylinder with 76-mm thick walls. A hydraulic spray nozzle provided a mist which washed the fibers. The design efficiency was 99% at 0.47 m^3/s, with a 1500-Pa pressure drop. Large particles were collected by impaction and interception. Small particles were removed with good efficiency by diffusion.

Ancillary Equipment. Two standard HEPA filters were located downstream of the fibrous scrubber. An exhaust fan, duct, flow control equipment, and instrumentation (temperature, pressure, aerosol characterization) completed the test system.

* Spraying System Co., Wheaton, Illinois.

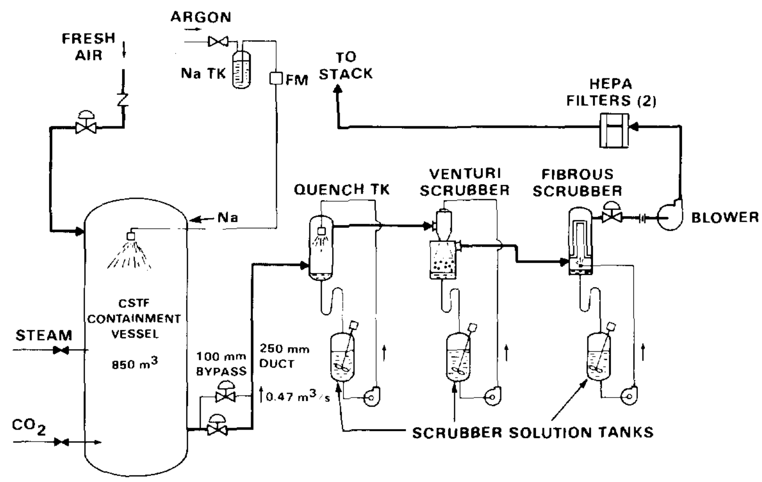

FIGURE 1. Flow Diagram of the CSTF Scrubber Air Cleaning System Used in Tests AC1-AC4. (Neg. 8010843 - 2)

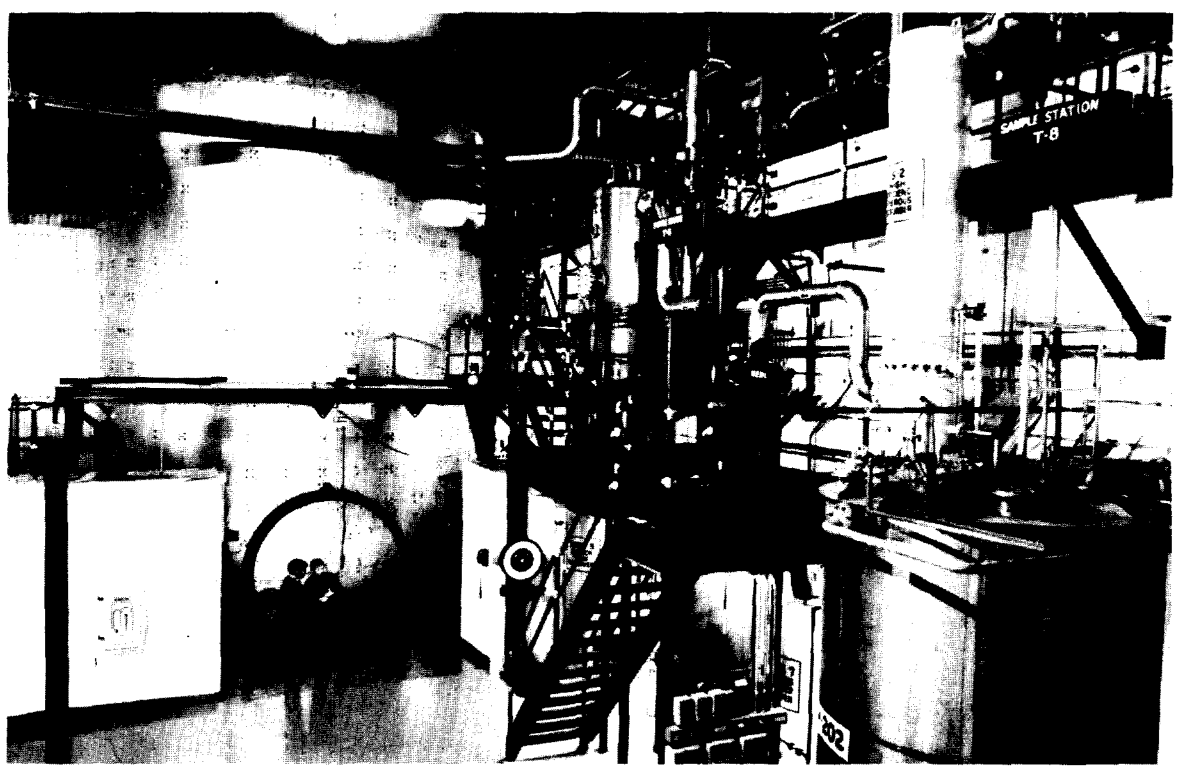

FIGURE 2. Photograph of Scrubber Air Cleaning System Installed in the CSTF. (Neg. 7813233-12 cn)

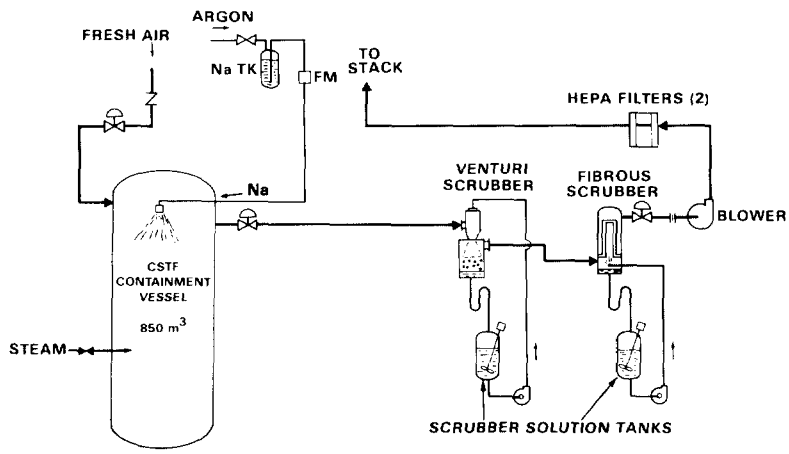

FIGURE 3. Flow Diagram of the CSTF Scrubber Air Cleaning System Used in Tests AC-5 and AC-6. (Neg. 8010843-3)

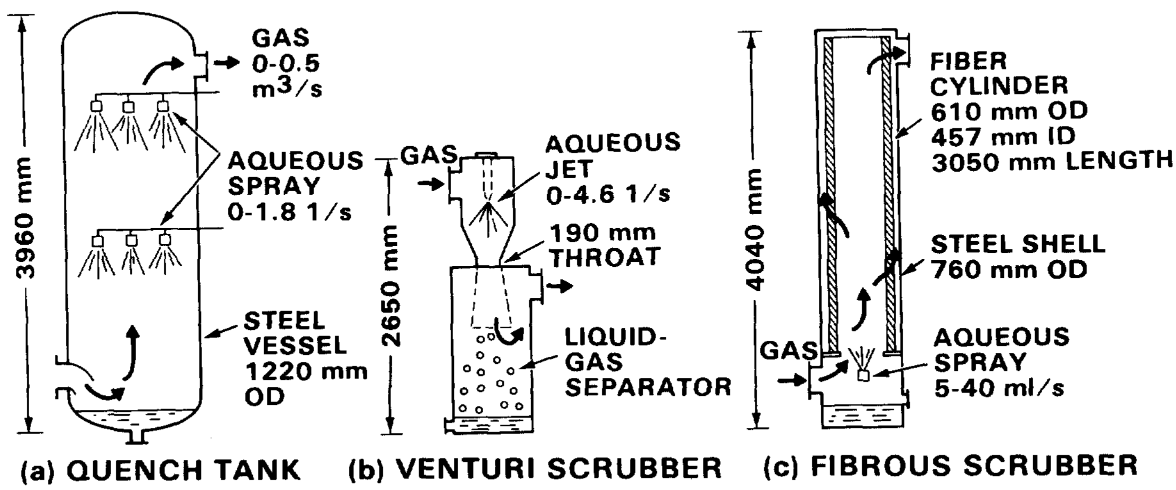

FIGURE 4. Details of CSTF Aqueous Scrubber Components. (Neg. 8010845-1)

Test Procedure

Sodium was sprayed continuously into the air atmosphere within the sealed CSTF containment vessel (CV). After conditions had stabilized, the CV was vented through the scrubbers, reducing the CV pressure from 70 kPa to zero with ∿ 16 minutes. The vent flow rate was controlled at 0.47 std. m^3/s by a butterfly valve in the 260-mm diameter duct leading from the CV to the scrubbers. When the pressure was nearly zero, the exhaust fan was started and the flow rate was controlled by an orifice meter and downstream valve for the duration of the test. When the CV pressure became slightly negative, a CV inlet valve was opened to provide the source of purge air. Aerosol samples were taken periodically from four locations in the CV and upstream and downstream of each scrubber component. Liquid from each of the three scrubber tanks was sampled periodically. The gas and liquid flow rates to the scrubbers were varied. At the end of the test, the downstream HEPA filters were destructively analyzed for sodium and iodine. All vessels and equipment were washed and a material balance was made. Samples were analyzed for sodium by acid titrimetry or flame emission spectrometry. NaI analyses were by colorimetry.

Test Conditions

The test conditions are summarized in Table I. The chief differences between tests were the type of air cleaning systems, the type of test aerosol, and the sodium spray rate.

III. Experimental Results

Test Aerosol Properties

Knowledge of the properties of the test aerosol was important for a meaningful evaluation of the performance of the air cleaning equipment. Approximately 400 samples were taken during each test to characterize the aerosol as to size distribution, suspended mass concentration and chemical composition. The aerosol properties are summarized in Table II. The aerosol was typical of that produced in earlier sodium pool fires and sodium spray tests in the CSTF.[5,6]

Thermal Hydraulic Performance

The hot gas from the containment vessel was cooled effectively when the design flow rates of gas and liquid were used. Table III shows that the combination of quench tank and venturi brought the gas leaving the venturi scrubber to essentially thermal equilibrium with the liquid leaving the venturi (< 1°C difference). When the quench tank was removed, the venturi was not able to cool the gas as well, but cooling was adequate (2.2°C difference between exit gas and liquid) when the ratio of liquid to gas flow

TABLE I. Test Conditions

	AC1	AC2	AC3	AC4	AC5	AC6
Air Cleaning System Components[(a)]	QT,VS,FS	QT,VS,FS	QT,VS,FS	QT,VS,FS	VS, FS	VS, FS
Dominant Aerosol Chemical Form	Na_2O_2	NaOH	Na_2CO_3	Wet NaOH	NaOH	NaOH
Na spray rate, avg, g/s	5.47	6.98	4.14	5.13	9.36	24.3
Duration of Na Spray, min	2145	1830	2200	2490	2175	770
Total Na Sprayed, kg	704	766	547	767	1220	1125
Steam flow to CV, avg, g/s	0	5.0	4.5	4.3	4.0	5.9
CO_2 flow to CV, avg, g/s	0	0	11.0	0	0	0
Dewpoint in CV atmos., avg, °C	-10	21	20	10	1.0	9
Gas flowrate to scrubbers, avg, std. m^3/s[(b)]	0.103	0.204	0.153	0.371	0.367	0.361
Total gas to scrubbers, std. m^3	10,100	17,480	17,990	48,200	36,680	15,660
Total aerosol vented/purged, kg Na	37.6	128.0	42.8	118.6	284.3	219.9
Total NaI to scrubbers, g NaI	0	0	686.6	429.8	0	0

(a) QT = quench tank, VS = venturi scrubber, FS = fibrous scrubber.

(b) Standard temperature and pressure, 0°C, 0.101 MPa absolute.

TABLE II. Aerosol Properties

	AC1	AC2	AC3	AC4	AC5	AC6
Suspended conc.,[a] g Na/m^3 STP[b]						
Average	4.66	9.74	2.38	2.46	10.8	22.5
Maximum	15.2	20.7	13.5	14.1	12.6	26.8
Aerosol AMMD[c], μm						
Average	3.1	3.7	3.3	3.5	3.3	5.5
Maximum	4.4	6.4	6.5	5.3	3.8	6.0
Aerosol geometric std. dev., σ_g						
Assoc. with average size	2.8	2.1	2.8	2.3	2.5	2.5
Assoc. with maximum size	2.7	2.2	2.7	2.3	2.4	2.2
Sodium fraction, g Na/g	0.515	0.437	0.434	0.25	0.558	0.458

(a) Sodium only. Divide by sodium fraction to obtain total aerosol mass.
(b) Standard temperature and pressure, 0°C, 0.101 MPa.
(c) Aerodynamic mass median diameter.

rates was at least 0.0056. It is important that the gas entering the fibrous scrubber be saturated so that a negligible fraction of the fibrous scrubber liquid spray is evaporated. An L/G ratio of 0.007 (volume basis) is recommended for the venturi for plant applications.

The maximum pressure drop measured across each scrubber during the tests is listed in Table III for a nominal gas flow rate of 0.47 std. m^3/s (1000 SCFM). The pressure drop across each component varies linearly with gas flow rate. Typical measurements using room temperature air are shown in Figure 5. Slightly higher pressure drops were measured during tests due to the effects of aerosol and NaOH in the liquid. Because the eductor type venturi induces a positive pressure by the pumping action of the liquid jet, the total pressure differential across all three scrubbers is positive at gas flow rates less than 0.26 m^3/s (550 SCFM).

A high pressure drop across the fibrous scrubber was encountered during test AC-5 (5630 Pa, 22.5 in. H_2O) as a result of a combination of degraded operating conditions intentionally imposed on the air cleaning system. The conditions in test AC-5 which were outside the limits of design criteria were: gas flow rate 1.35 times design, venturi liquid flow rate 0.7 times design, fibrous liquid flow rate 0.14 times design, and NaOH concentration in the recirculated venturi liquid 1.8 times maximum. In addition, the liquid to the fibrous scrubber was stopped completely for 2 hr. The three-component system used in tests AC-1 - AC-4 could probably have handled these degraded conditions without causing the high pressure drop noted in test AC-5. During test AC-6, the design flow rates were used and the pressure drop was normal (1780 Pa, 7.1 in. H_2O) even though the aerosol concentration was approximately twice that in test AC-5.

Sodium Aerosol Removal Efficiency

The quantities of aerosol, expressed as sodium equivalent, retained by each scrubber, the inlet duct and the backup HEPA filter are listed in Table IV for each test. Actual masses were approximately twice the sodium values. The integrated removal efficiencies are also listed, as calculated from the mass deposited in each component. There was no significant difference attributable to the different aerosol forms. The differences that do appear are explainable by differences in system operating conditions or aerosol mass concentration and particle size. For example, liquid flow to the quench tank was shut off for eight hours in test AC-4, causing the low efficiency of 37.9% compared to an average of 69.0% in the other three tests where a QT was used. Likewise, the high venturi efficiency of 94.5% in test AC-6 was due to the larger aerosol particle sizes generated in test AC-6.

TABLE III. Scrubber Temperature and Pressure Data[a]

	AC1	AC2	AC3	AC4	AC5	AC6
Quench Tank						
L/G x 1000[b]	2.2	2.1	1.7	1.5	(d)	(d)
Max. temp. of inlet gas, °C	268	313	256	154	(d)	(d)
Typical ΔT, exit gas and liquid, °C	8.3	8.9	4.4	9.4	(d)	(d)
Max. pressure drop, Pa	80	80	80	80	(d)	(d)
Venturi Scrubber						
L/G x 1000[b]	5.4	5.4	5.4	5.4	4.3	5.6
Max. temp. of inlet gas, °C	50	64	58	54	150	223
Typical ΔT, exit gas and liquid, °C	0.7	0.2	0.3	0.0	8.4	2.2
Max. pressure drop, Pa[c]	-62	-25	-50	-125	-50	-320
Fibrous Scrubber						
L/G x 10^6[b]	8.8	9.1	9.1	9.1	9.4	71
Max temp. of inlet gas, °C	44	51	56	46	66	69
Typical ΔT, exit gas and liquid, °C	5.5	0	2.2	1.6	3.9	4.5
Max. pressure drop, Pa	1490	1600	1990	1920	5630	2100

(a) At nominal gas flow rate of 0.47 std. m^3/s (1000 SCFM).

(b) Ratio of gas to liquid volumetric flow rates, based on inlet conditions.

(c) Minus sign indicates a pressure gain.

(d) Not applicable.

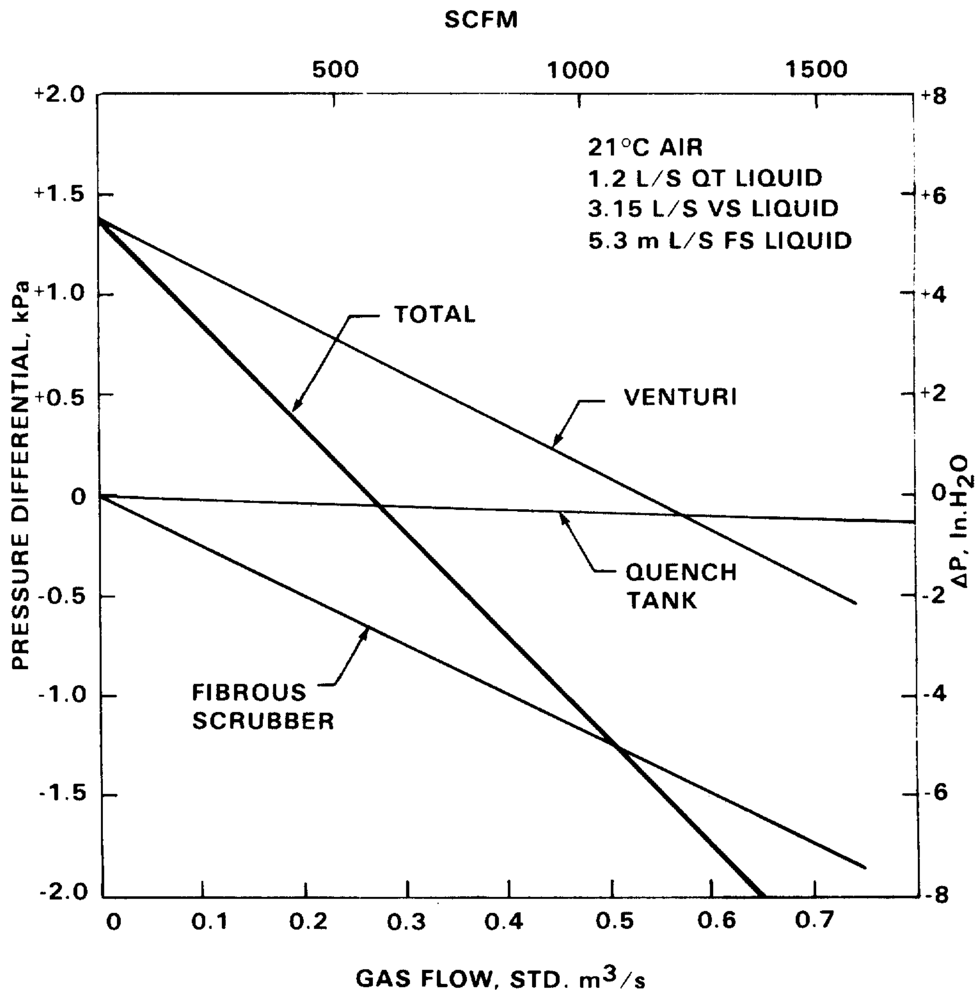

FIGURE 5. Differential Pressure Across Three-Component Scrubber System. (Neg. 8010843-1)

TABLE IV. Sodium Aerosol Removal Efficiency Based on Post-Test Material Balance

Component	Test AC1		Test AC2		Test AC3	
	Mass Collected kg Na	Average Removal Efficiency %	Mass Collected kg Na	Average Removal Efficiency %	Mass Collected kg Na	Average Removal Efficiency %
Inlet Duct	6.420	17.0	53.616	41.9	16.252	37.9
Quench Tank	24.805	79.4	48.774	65.9	16.389	61.6
Venturi Scrubber	5.728	89.2	22.681	88.5	8.793	86.1
Fibrous Scrubber	0.6852	98.6	2.931	91.1	1.407	99.1
HEPA Filter	0.0097	(a)	0.0282	(a)	0.012	(a)
Total	37.6479	99.97(b)	128.0302	99.96(b)	42.853	99.95(b)

Component	Test AC4		Test AC5		Test AC6	
	Mass Collected kg Na	Average Removal Efficiency %	Mass Collected Kg Na	Average Removal Efficiency %	Mass Collected kg Na	Average Removal Efficiency %
Inlet Duct	15.638	13.2	18.020	6.34	25.486	11.6
Quench Tank	39.000	37.9	(c)	(c)	(c)	(c)
Venturi Scrubber	55.325	86.5	215.108	80.8	183.660	94.5
Fibrous Scrubber	8.525	99.2	51.113	99.9	10.675	99.3
HEPA Filter	0.071	(a)	0.049	(a)	0.070	(a)
Total	118.559	99.93(b)	284.290	99.98(b)	219.891	99.96(b)

(a) Not measured, assumed 100%
(b) Excluding duct and HEPA
(c) Not applicable

It is interesting to note that the average sodium removal efficiency for the 2-component system used in tests AC-5 and AC-6 compared very closely with the average values for the 3-component system used in tests AC-1 through AC-4, as shown in Table V. The slightly higher efficiencies observed for the 2-component system was due chiefly to the higher aerosol concentration and particle size used in those tests.

TABLE V. Comparison of Three- and Two-Component Scrubber Systems

	3-Scrubber System[(a)]		2-Scrubber System[(b)]		All Six Tests	
	Total Mass kg Na	Average Effic. %	Total Mass Kg Na	Average Effic. %	Total Mass kg Na	Average Effic. %
Inlet Duct	91.93	27.5	43.51	9.0	135.43	21.3
Quench Tank	128.96	61.2	(c)	(c)	128.97	61.2
Venturi Scrubber	92.53	87.6	398.76	87.7	491.29	87.6
Fibrous Scrubber	13.55	99.0	61.79	99.6	75.34	99.2
	326.97	99.952[(d)]	504.06	99.97[(d)]	831.03	99.958[(d)]

(a) Tests Acl through AC4.

(b) Tests AC-5 and AC6

(c) Not applicable

(d) Excluding duct and HEPA

Instantaneous efficiencies were calculated at approximately hourly periods by taking aerosol samples from scrubber inlets and outlets. The average values of all the aerosol based efficiencies are listed in Table VI along with the average efficiencies based on post-test material balance. The excellent agreement between the two methods gives added confidence to the efficiency calculations. The aerosol-based values are believed to be more accurate for any given operating period, while those based on post-test material balance are more accurate for overall efficiencies.

Aerosol Deposition in Ducts

A significant fraction of the aerosol deposited in the duct leading to the scrubber, as shown in Tables IV and V. In order to obtain additional information on potential plugging of ducts by deposited aerosol, several small diameter ducts were used in parallel with the main 265-mm diameter ducts. A summary of aerosol deposition and plugging is presented in Table VII. Some effects of chemical and physical nature were noted, with wet NaOH sticking to the walls and dry oxide and carbonate being resuspended. But the chief factor in determining whether the duct plugged was the diameter. The data of Table VII are plotted as a graph of the mass of aerosol entering the duct as a function of duct diameter in Figure 6. Four of the smaller ducts were plugged, as defined by the point where gas flow rate was reduced to less than 25% of its initial value at a pressure drop of 7.5 kPa (30 in. H_2O). Insufficient aerosol entered the remaining ducts to cause plugging. The curve in Figure 6 is a visual fit of the four data points where plugging occurred and can be represented by the following equation:

$$m = 4.0 \times 10^4 \, d^3 \qquad [1]$$

where m = mass of aerosol entering duct, kg
d = duct internal diameter, m

The area above the curve represents conditions where duct plugging can be expected. The area below the curve represents conditions where plugging is not expected. Obviously, Equation [1] greatly oversimplifies the solution to a complex problem and is based on only a few data points. However, the d^3 relationship agrees with theoretical reasoning by Vaughan.(7)

NaI Vapor Removal

Sodium iodide vapor was injected into the 265-mm diameter inlet duct just upstream of the quench tank in tests AC-3 and AC-4 by passing hot argon through a furnace containing molten NaI. The NaI vapor line was heated to ∿850°C to keep the argon stream unsaturated until it merged with the cooler gas stream from the containment vessel. The aerosol and liquid samples were analyzed for iodine and removal efficiencies were calculated by the same procedure used for sodium efficiencies. The NaI removal efficiencies determined by post-test material balances are listed

TABLE VI. Comparison of Sodium Aerosol Removal Efficiencies Measured by Aerosol and Liquid Sampling

Test No.	Quench Tank		Venturi Scrubber		Fibrous Scrubber		Total System	
	Aerosol(a) Sampling	Liquid(b) Sampling	Aerosol(a) Sampling	Liquid(b) Sampling	Aerosol(a) Sampling	Liquid(b) Sampling	Aerosol(a) Sampling	Liquid(b) Sampling
AC1	82.1	79.4	75.7	89.2	97.43	98.60	99.92	99.97
AC2	77.5	65.6	95.2	88.5	99.14	99.05	99.99	99.96
AC3	71.9	61.6	92.7	86.1	99.34	99.15	99.99	99.95
AC4	56.3	37.9	77.8	86.5	99.20	99.17	99.91	99.93
AC5	(c)	(c)	81.9	80.8	99.80	99.90	99.98	99.98
AC6	(c)	(c)	86.5	94.5	99.56	99.35	99.95	99.96
Average	72.0	61.2	85.0	87.6	99.08	99.20	99.96	99.96

(a) Average of ∿35 aerosol sampling periods.

(b) From post-test material balance.

(c) Not applicable.

TABLE VII. Summary of Aerosol Deposition in Ducts

Duct Number	Dimensions: I.D. mm	Dimensions: Length m	Aerosol Mass, kg[(a)]: Deposit In Duct	Aerosol Mass, kg[(a)]: Penetrated Duct	Aerosol Mass, kg[(a)]: Total	% Pen.	Na Fraction g Na per g Total	Bulk Denisty g/cm^3	Max. ΔP kPa	Duct Plugged
AC1-10	265	16.4	12.5	60.8	73.3	82.9	0.515	0.16	0.5	No
AC2-1	22.1	14.6	0.516	<0.03	0.516	<5	0.437	~0.5	70	Yes
AC2-10	265	16.4	122	172	294	58.5	0.437	0.87	2.8	No[(b)]
AC3-1	22.1	13.3	0.275	0.110	0.385	28.6	0.434	0.11	70	Yes
AC3-2	52.5	13.5	0.420	0.405	0.825	49.1	0.434	0.11	9.0	No
AC3-10	265	16.4	37.0	61.7	98.7	62.5	0.434	0.11	0.87	No
AC4-2	52.5	13.5	0.137	4.37	4.51	96.9	0.25	~0.6	5.2	No
AC4-10	265	16.4	62.6	455	518	87.8	0.25	~0.6	3.3	No
AC5-2	52.5	17.8	3.56	2.60	6.16	42.2	0.558	~0.5	70	Yes
AC5-4	110	21.3	20.4	50.8	71.2	71.3	0.558	~0.5	7.5	Yes
AC5-10	265	10.7	27.8	541	569	95.1	0.558	~0.5	1.0	No
AC6-10	265	10.7	55.6	424	480	88.3	0.458	0.64	4.2	No

(a) Determined by analyzing for Na and dividing by Na mass fraction.

(b) Duct plugged post-test by heating duct walls above NaOH melting point.

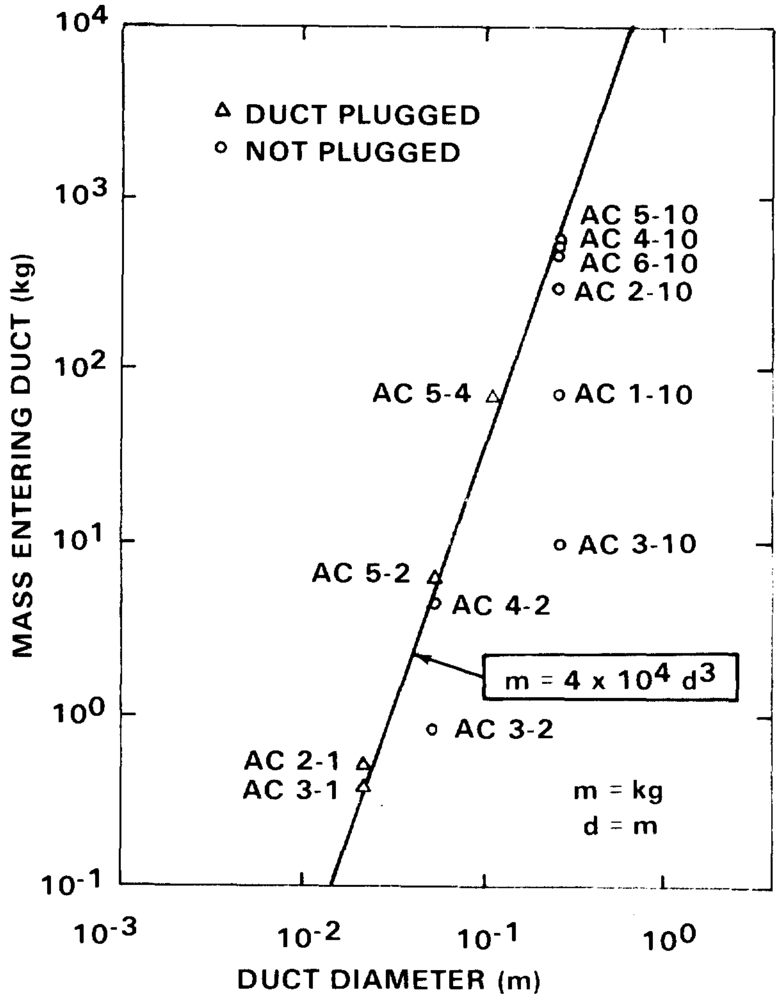

FIGURE 6. Duct Plugging as a Function of Duct Diameter. (Neg. 801843-4)

in Table VIII. The lower efficiency found in test AC-4 corresponds to the higher gas flow rate used in test AC-4. The NaI efficiencies were considerably lower than that of the sodium aerosol, as expected, due to their very small size and short time available for agglomeration. However, the fibrous scrubber was effective in collecting ∿99% of the NaI mass.

TABLE VIII. NaI Removal Efficiency Based on Post-Test Material Balance

	Test AC3		Test AC4	
	Mass Collected g NaI	Average Removal Efficiency %	Mass Collected g NaI	Average Removal Efficiency %
Quench Tank	198.1	28.8	42.15	9.7
Venturi Scrubber	205.9	42.0	42.51	10.8
Fibrous Scrubber	282.6	99.47	344.11	98.46
HEPA Filter	1.51	(a)	5.389	(a)
Total	688.1	99.78(b)	434.159	98.76(b)

(a) Not measured. Assumed 100%.

(b) Excluding HEPA filter.

IV. Summary and Conclusions

The six tests described in this paper provide a convincing demonstration of the feasiblity of using a venturi-fibrous scrubber system to remove aerosol from vented and purged containment atmospheres under conditions postulated for severe LMFBR accidents. During these tests, 146,000 std. m³ of gas at temperatures up to 313°C and containing ∿ 1700 kg of aerosol mass was cleaned with only ∿ 0.5 kg total penetration of the scrubbers. Specific conclusions are:

- The overall sodium removal efficiency for all six tests averaged 99.96%. The efficiency was remarkably insensitive to widely varying operating conditions, a feature resulting from the use of a multi-component air cleaning system.

- The efficiency of a 2-component system comprised of an eductor venturi and a high efficiency fibrous scrubber was equal to that of a 3-component system comprised of the same two components plus a pre-cooler spray chamber (quench tank). However, the 2-component system was more sensitive to thermal and flow conditions.

- Essentially no differences in removal efficiency were observed for four chemical forms of sodium aerosol. The chief parameters affecting efficiency were the particle size and the gas flow rate.

- Higher efficiencies were noted for lower gas velocities, a favorable feature for use with variable flow rates anticipated for vented containment operations.

- Aerosol deposition in ducts leading to the scrubbers should be considered for any plant application. An empirical correlation is established for plugging of ducts.

- The removal efficiency for freshly nucleated NaI particle averaged 99.3%. Although lower than that of aged sodium fire aerosol, this is considered good removal of particles in a difficult size range for many types of air cleaning equipment.

- Control of containment venting and purging flow rates by 260-mm butterfly valves was satisfactory.

- The total mass loading capability of the system depends on the quantity of water provided. A concentration limit of 5-molar NaOH is recommended so that solubility limits will not be exceeded.

V. References

1. R. K. Hilliard, J. D. McCormack and A. K. Postma, "Evaluation of Air Cleaning System Concepts for Emergency Use in LMFBR Plants," HEDL-TME 76-41, Hanford Engineering Development Laboratory (1976).

2. A. K. Postma, R. K. Hilliard, "Nucleation and Capture of Condensible Airborne Contaminants in an Aqueous Scrubbing System," HEDL-TME 78-82, Hanford Engineering Development Laboratory (September, 1978).

3. R. K. Hilliard, et.a., "Containment Air Cleaning for LMFBRs" in Proc. of the International Meeting on Fast Reactor Safety Techology, Seattle, Washington, Am. Nucl. Soc., August 19-23, 1979.

4. R. K. Hilliard, et.a., "Sodium Oxide/Hydroxide Aerosol Properties and Behavior in a Large Vessel," in Proc. of the 15th DOE Nuclear Air Cleaning Conference, CONF - 780819, p. 764 (1979).

5. R. K. Hilliard, J. D. McCormack, and A. K. Postma, "Aerosol Behavior During Sodium Pool Fires in a Large Vessel - CSTF Tests AB1 and AB2," HEDL-TME 79-28, Hanford Engineering Development Laboratory (1979).

6. J. D. McCormack, R. K. Hilliard, A. K. Postma and R. K. Owen, "Aerosol Behavior During Sodium Spray Fires and Comparison with Computer Codes," in Proc. of the International Meeting on Fast Reactor Safety Technology, Seattle, Washington, Am. Nucl. Soc., August 19-23, 1979.

7. E. U. Vaughan, "Simple Model for Plugging of Ducts by Aerosol Deposits," Trans. Am. Nucl. Soc., 28, 507 (1978).

DISCUSSION

FREEMAN: As a result of your work, could you hazard a guess as to life expectancy of the deep-bed filter and the HEPA filters downstream?

McCORMACK: The HEPA filters see practically no aerosol burden. We would remove them at the end of each run and analyze them destructively for sodium to obtain our overall efficiencies and, typically, we might have 30 to 40 grams on a HEPA filter. The temperatures there were warm enough to maintain the aerosol in a dry state. I guess we did not see any degradation in the 30 to 60-hour test that we ran. With reference to the life of the polypropylene demister, it is a litter harder to say. We ran a series of increasing temperature tests at the end of this test series that we did not talk about in our paper. We ran pressure drops versus time at several temperatures. At approximately 210°F we started to see degradation of the bed material in about a week's time. So it appeared to us there was a very definite limit to the bed temperature for this application.

FREEMAN: How about the aerosols? Were they all soluble?

McCORMACK: Yes, we used only soluble sodium aerosols.

SHAVER: I enjoyed your paper. I recall a number you mentioned of 60 gallons per minute in your venturi scrubber. In an actual installation, where you might have some contamination, it seems that we would have a pretty high flow rate. What do we do with the liquid that passes on?

McCORMACK: That is a lot of water. We recycle the water and make up for evaporation losses. A substantial fraction of the cooling of the gas stream is by evaporation at the venturi scrubber. We suggest that concentrations be limited to approximately 5 molar in a system. Therefore, the designer has to anticipate the amount of sodium hydroxide he will have and provide that much water plus makeup water. We suggest recycling the water. We do not address the problems of subsequent disposal of the water.

ANON.: Regarding the chemical forms of sodium, did you take into account the heat of reaction in the water? If you have a large amount of sodium aerosol, there will be an enormous heat of reaction.

McCORMACK: Yes, that is very true. We didn't have to take account of it in our experiments, but designers generally do allow for the heat of reaction and make appropriate provisions for the amount of evaporation.